Supporting Information

P_2S_5 Reactive Flux Method for the Rapid Synthesis of Mono- and Bimetallic 2D Thiophosphates $M_{2-x}M'_xP_2S_6$

Daniel G. Chica,[1] Abishek K. Iyer,[1] Matthew Cheng,[2] Kevin M. Ryan,[3] Patrick Krantz,[3] Craig Laing,[1] Roberto dos Reis,[2,4] Venkat Chandrasekhar,[3] Vinayak P. Dravid,[2,4,5] Mercouri G. Kanatzidis[1,*]

[1]*Department of Chemistry, Northwestern University, Evanston, Illinois, 60208*

[2]*Department of Material Science and Engineering, Northwestern University, Evanston, Illinois, 60208*

[3]*Department of Physics and Astronomy, Northwestern University, Evanston, Illinois, 60208*

[4]*Northwestern University Atomic and Nanoscale Characterization Experimental (NUANCE) Center, Northwestern University, Evanston, Illinois, 60208*

[5]*International Institute for Nanotechnology (IIN), Northwestern University, Evanston, Illinois, 60208*

*Corresponding author

Supplemental Experimental Information

Powder X-ray diffraction

The powder diffraction patterns were collected on a Rigaku Miniflex 600 diffractometer with a Cu Kα source operating at 40 kV and 15 mA with a Kβ filter. Preferred orientation was reduced by sieving the lightly ground samples to a particle size of <53 μm and using a welled, zero background sample holder. Simulated powder pattern were made using Mercury 4.0.[1] The lattice parameters were determined using Rietveld refinement through GSAS II.[2]

Variable temperature powder X-ray diffraction

In a nitrogen filled glovebox, the same mass of reagents used for bulk synthesis were combined in an agate mortar and pestle and ground for 10 min. The powder was loaded into a 0.5 mm fused silica capillary and flame sealed under 3×10^{-3} mbar. Variable temperature diffraction patterns were collected on a STOE STADI – MP diffractometer. The capillary was placed in the furnace attachment which has temperature stability of 0.1°C. This diffractometer uses an asymmetric curved Germanium monochromator to select the Mo $K\alpha_1$ line (λ = 0.70930 Å) and has a one-dimensional silicon strip detector (MYTHEN2 1K, DECTRIS). The X-ray generator operates at 50 kV and 40 mA. Prior to measurement, calibration was performed using a NIST silicon standard (640d). The heating profile used can be seen in Figure S30.

Scanning electron microscopy and energy dispersive X-ray spectroscopy

SEM images were collected using Hitachi S-3400N-II. The accelerating voltage and probe current were set to 20 keV and 70 mA, respectively. The energy dispersive X-ray spectra were collected using an Oxford INCAx-act EDS system. The spectra were analyzed using Oxford Instruments AZtec software.

Diffuse reflectance UV/Vis. Spectroscopy

The reflectance spectra were collected using a Shimadzu UV-3600 PC double-beam, double-monochromator spectrophotometer. The baseline was collected using $BaSO_4$. Powder samples made from **Heating 1** were pressed onto compressed $BaSO_4$ powder. The reflectivity data was

converted to absorbance data using the Kubelka-Munk equation, $\alpha/S = (1-R)^2/2R$, where α and S are the absorption and scattering coefficients, respectively and R is the reflectance .[3]

Table S1. Mass of reagents used for the flux reactions.

Compound	Primary metal mass (moles)	Secondary metal mass (moles)	P_2S_5 mass (moles)
$Mn_2P_2S_6$	0.2829 g (5.150 mmol)	N/A	1.7171 g (7.725 mmol)
$Fe_2P_2S_6$	0.2869 g (5.138 mmol)	N/A	1.7131 g (7.707 mmol)
$Co_2P_2S_6$	0.3004 g (5.098 mmol)	N/A	1.6996 g (7.646 mmol)
$Ni_2P_2S_6$	0.2994 g (5.101 mmol)	N/A	1.7006 g (7.651 mmol)
$Zn_2P_2S_6$	0.3279 g (5.015 mmol)	N/A	1.6721 g (7.523 mmol)
$Cd_2P_2S_6$	0.5043 g (4.486 mmol)	N/A	1.4957 g (6.729 mmol)
$MnFeP_2S_6$	Mn: 0.1413 g (2.572 mmol)	Fe: 0.1436 g (2.572 mmol)	1.7151 g (7.716 mmol)
$MnCoP_2S_6$	Mn: 0.1407 g (2.562 mmol)	Co: 0.1510 g (2.562 mmol)	1.7083 g (7.685 mmol)
$MnNiP_2S_6$	Mn: 0.1408 g (2.563 mmol)	Ni: 0.1504 g (2.563 mmol)	1.7088 g (7.688 mmol)
$FeCoP_2S_6$	Fe: 0.1429 g (2.559 mmol)	Co: 0.1508 g (2.559 mmol)	1.7063 g (7.676 mmol)
$FeNiP_2S_6$	Fe: 0.1429 g (2.559 mmol)	Ni: 0.1502 g (2.560 mmol)	1.7068 g (7.679 mmol)
$CoNiP_2S_6$	Co: 0.1503 g (2.550 mmol)	Ni: 0.1496 g (2.550 mmol)	1.7001 g (7.649 mmol)
$CuInP_2S_6$	Cu: 0.1504 g (3.266 mmol)	In: 0.2717 g (3.266 mmol)	1.5779 g (7.099 mmol)

$CuInP_2S_6$ (from elements)	Cu: 0.1504 g (3.266 mmol)	In: 0.2717 g (3.266 mmol)	P: 0.4398 g S: 1.1382 g (14.20 mmol) (35.50 mmol)
$Mg_2P_2S_6$	Mg: 0.1359g (5.591 mmol)	N/A	1.8641 g (8.386 mmol)

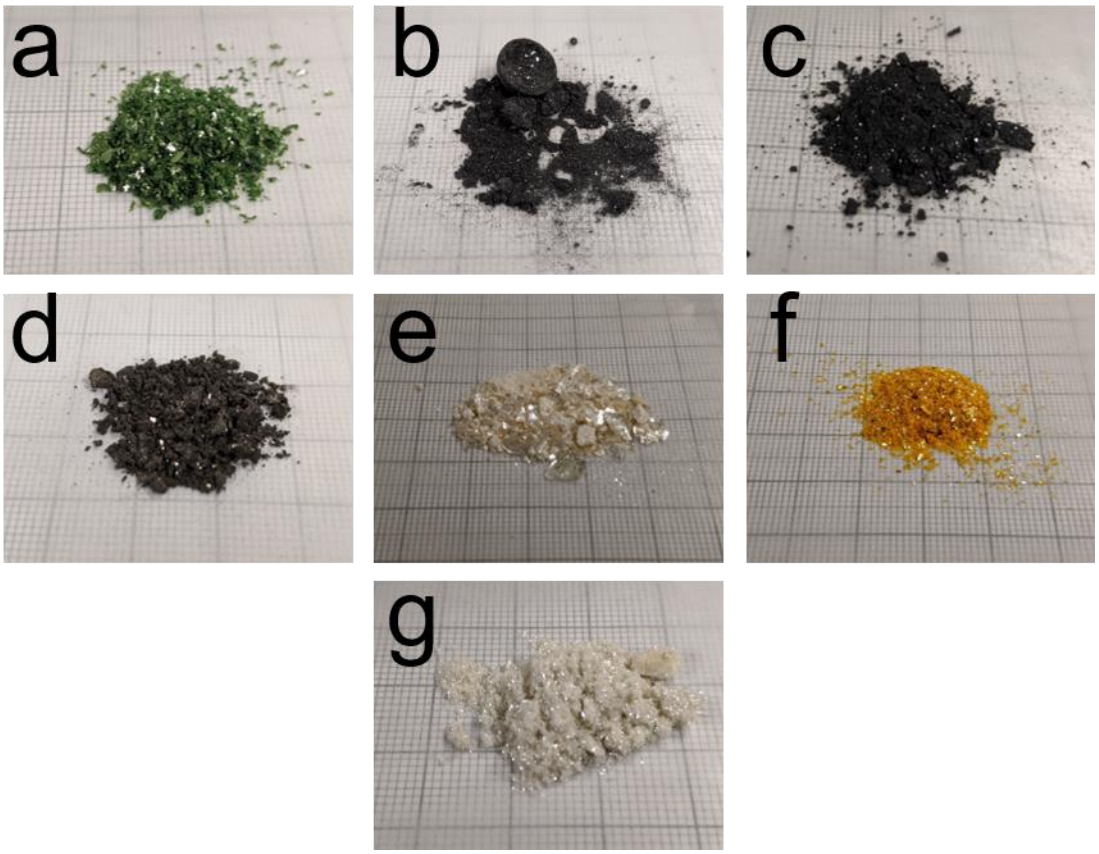

Figure S1. Bulk material made from the optimized synthesis, a.) $Mn_2P_2S_6$, b.) $Fe_2P_2S_6$, c.) $Co_2P_2S_6$, d.) $Ni_2P_2S_6$, e.) $Zn_2P_2S_6$, f.) $CuInP_2S_6$, g.) $Cd_2P_2S_6$. All the materials shown were synthesized using **Heating 1** except for $Co_2P_2S_6$ which was synthesized using **Heating 5**. The squares have an area of 1 mm^2.

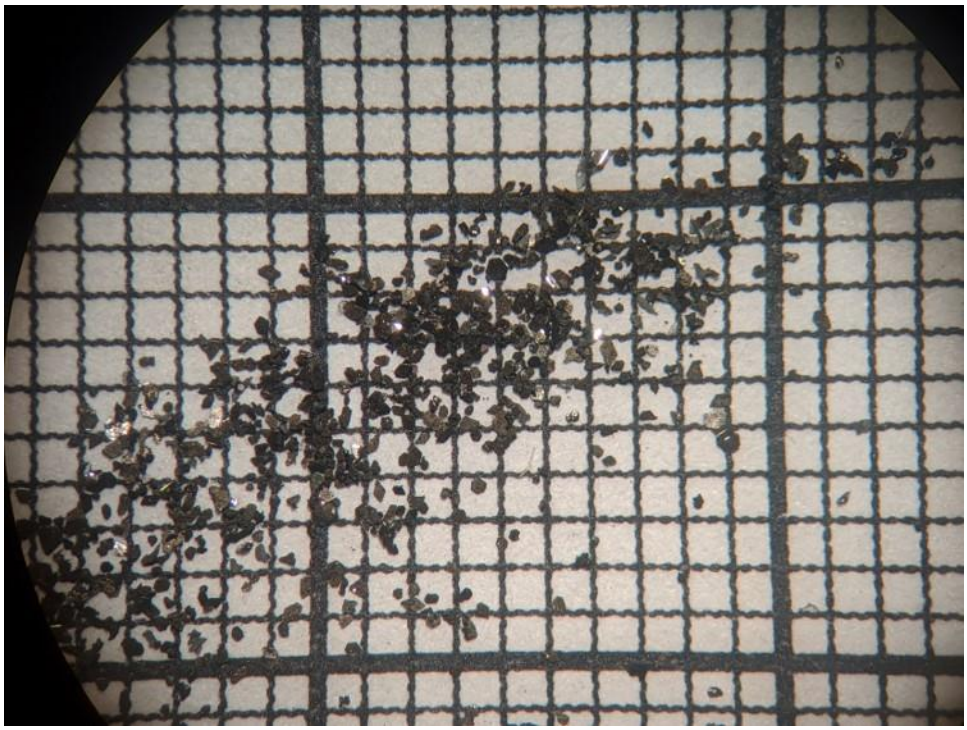

Figure S2. Largest $Ni_2P_2S_6$ crystals synthesized from **Heating 4**. The squares have an area of 1 mm^2.

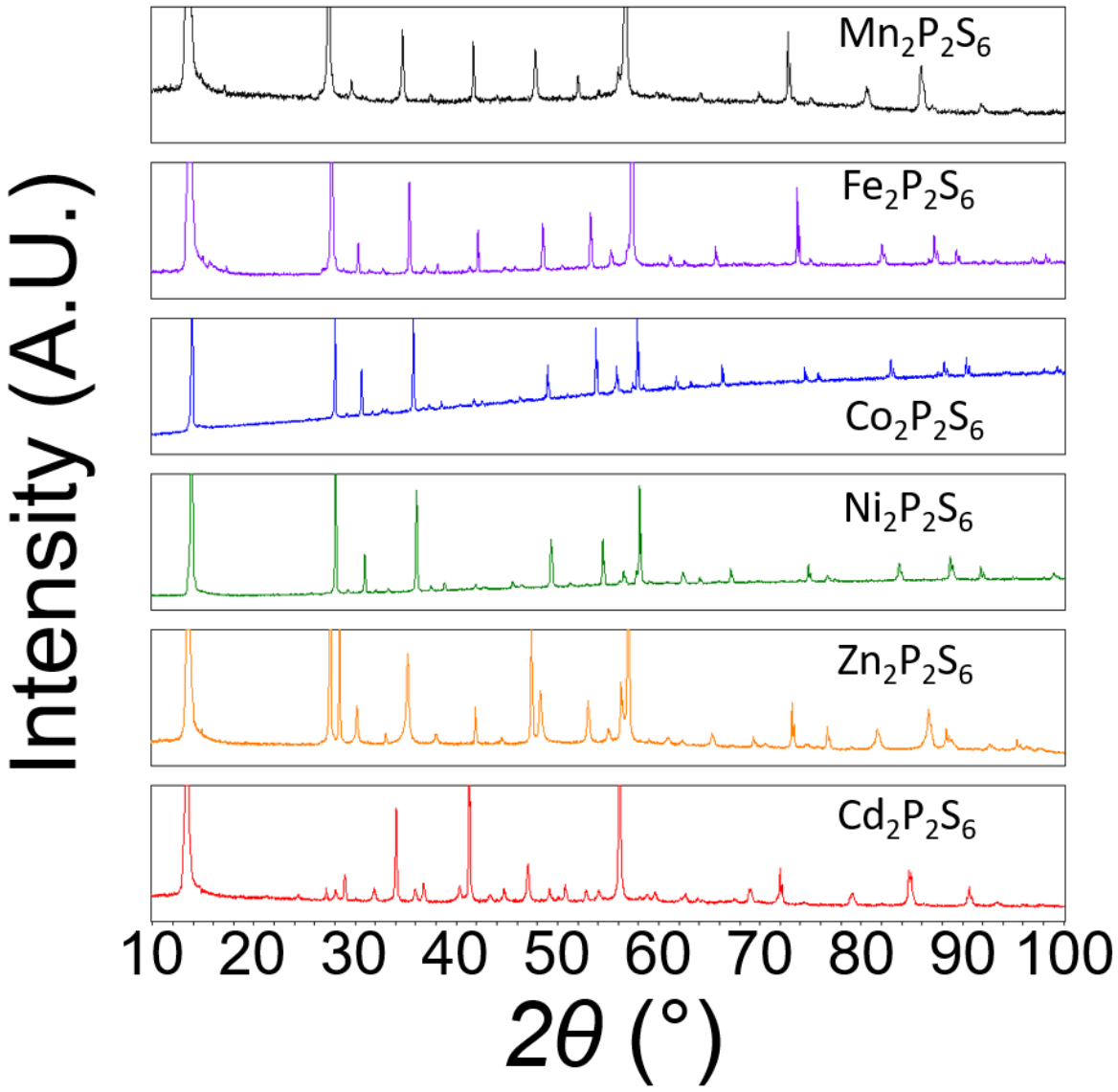

Figure S3. PXRD patterns of monometallics zoomed close to the baseline made from **Heating 1** except for $Co_2P_2S_6$ which was made from **Heating 5.**

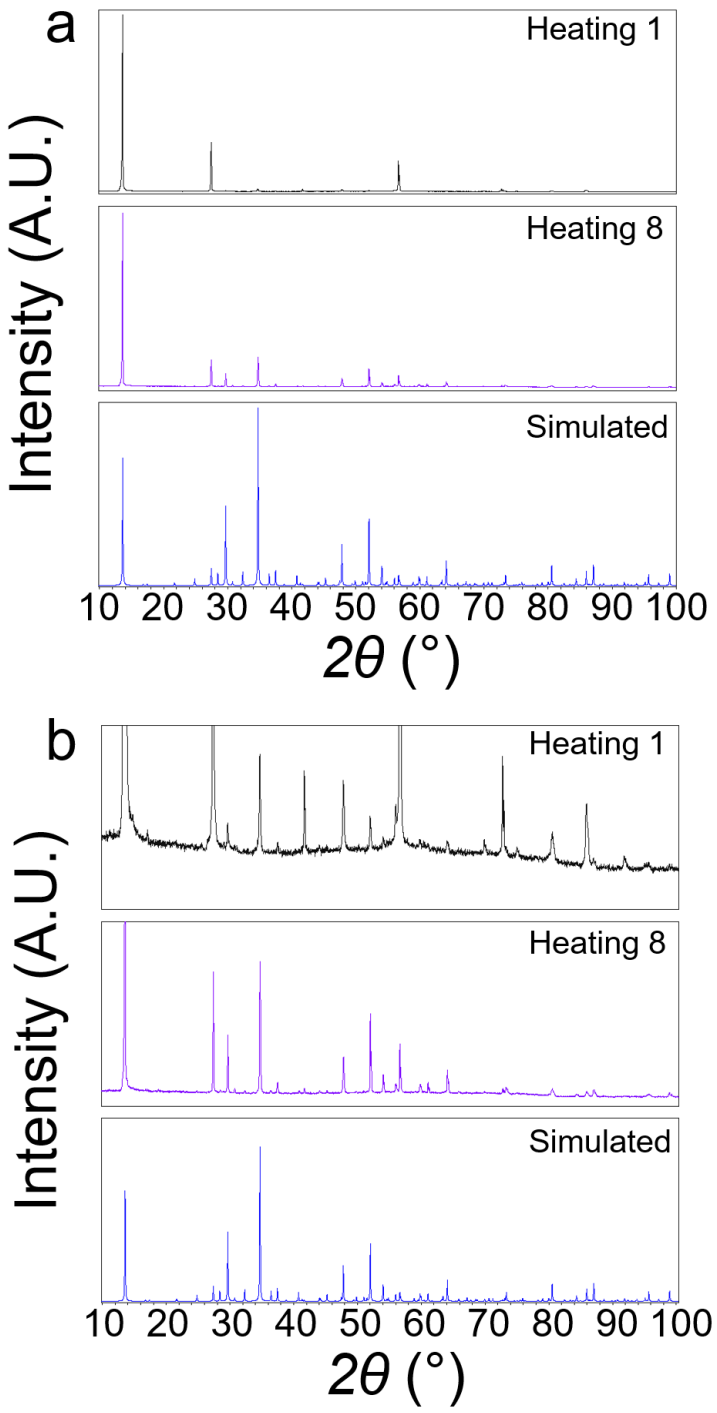

Figure S4. a.) Full range and b.) zoomed in PXRD patterns of $Mn_2P_2S_6$ made from **Heating 1**, **Heating 8**, and the simulated pattern. The discrepancy in peak intensity between the experimental and simulated PXRD patterns stems from preferred orientation, a common occurrence for layered materials.

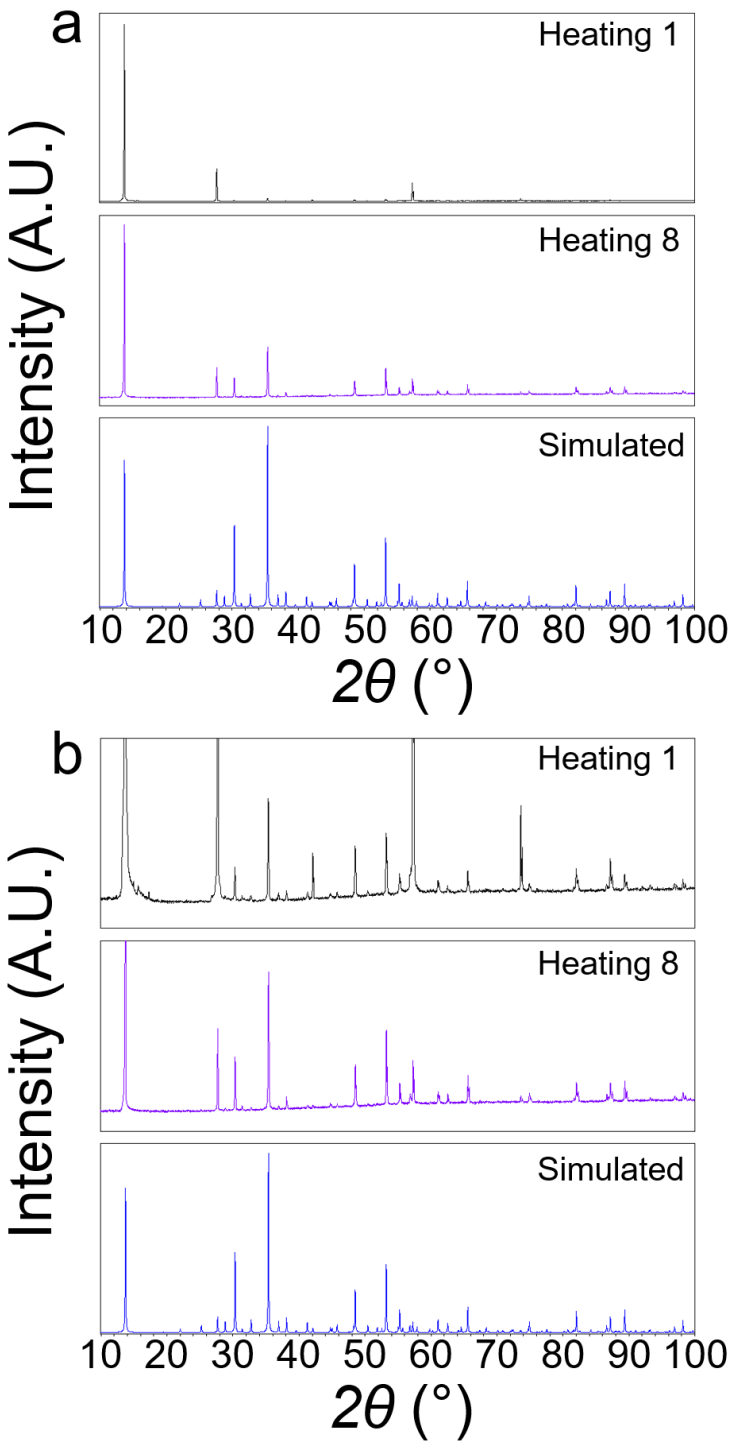

Figure S5. a.) Full range and b.) zoomed in PXRD patterns of $Fe_2P_2S_6$ made from **Heating 1**, **Heating 8**, and the simulated pattern. The discrepancy in peak intensity between the experimental and simulated PXRD patterns stems from preferred orientation, a common occurrence for layered materials.

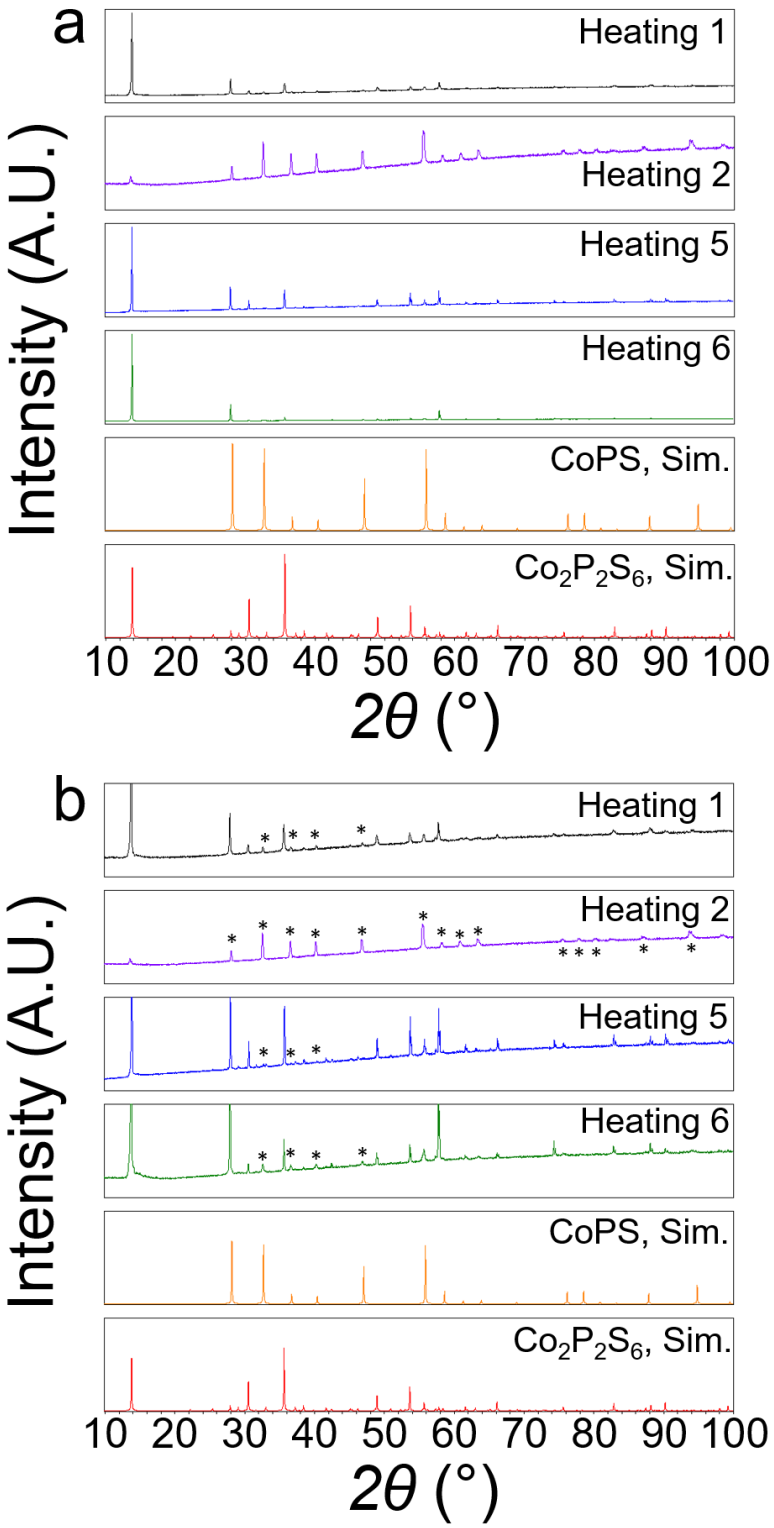
a
Heating 1
Heating 2
Heating 5
Heating 6
CoPS, Sim.
Co2P2S6, Sim.
Intensity (A.U.)
10 20 30 40 50 60 70 80 90 100
2θ (°)
b
Heating 1
Heating 2
Heating 5
Heating 6
CoPS, Sim.
Co2P2S6, Sim.
Intensity (A.U.)
10 20 30 40 50 60 70 80 90 100
2θ (°)

Figure S6. a.) Full range and b.) zoomed in PXRD patterns of $Co_2P_2S_6$ made from **Heating 1**, **Heating 2**, **Heating 5**, **Heating 6**, and the simulated patterns of CoPS and $Co_2P_2S_6$. The asterisks corresponds to the peaks from $Co(P,S)_2$. The discrepancy in peak intensity between the experimental and simulated PXRD patterns stems from preferred orientation, a common occurrence for layered materials.

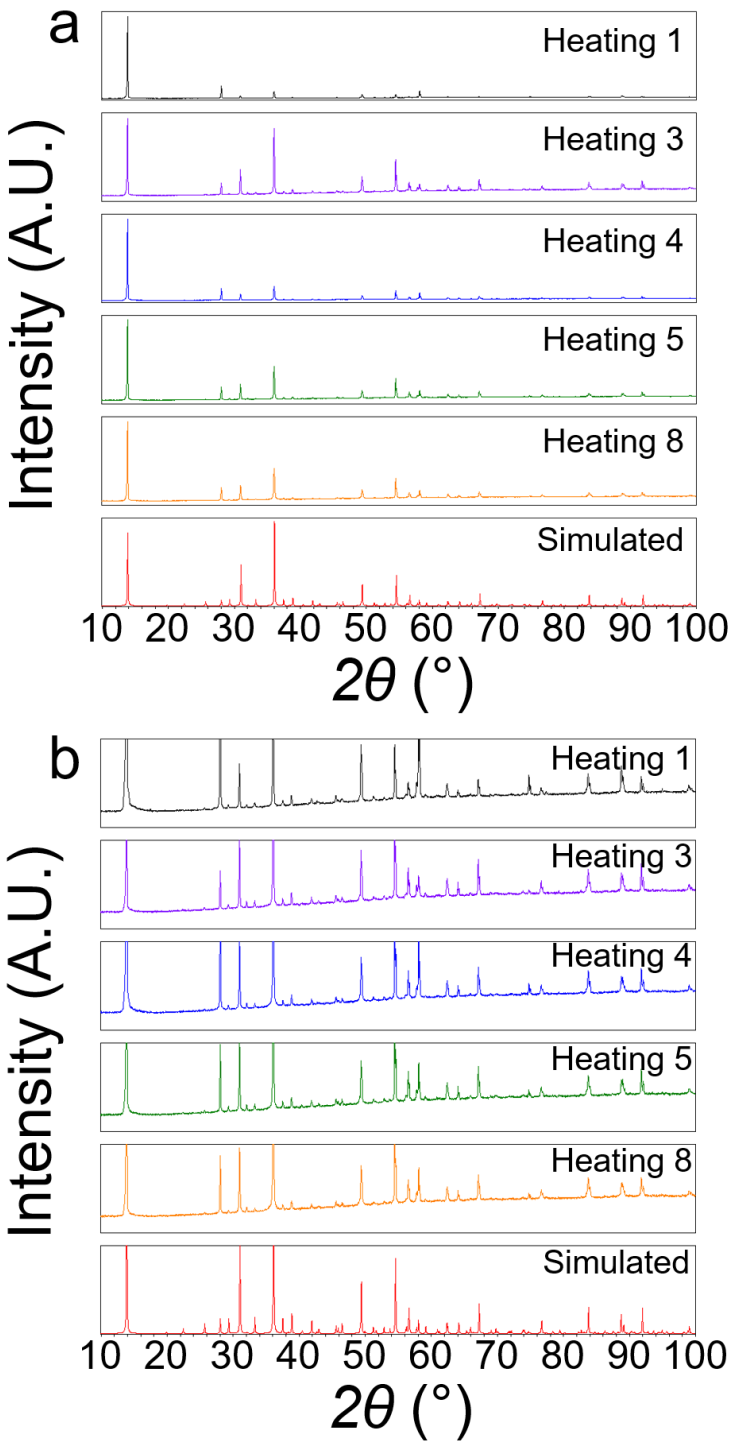

Figure S7. a.) Full range and b.) zoomed in PXRD patterns of $Ni_2P_2S_6$ made from **Heating 1**, **Heating 3**, **Heating 4**, **Heating 5**, **Heating 8**, and the simulated patterns. The discrepancy in peak intensity between the experimental and simulated PXRD patterns stems from preferred orientation, a common occurrence for layered materials.

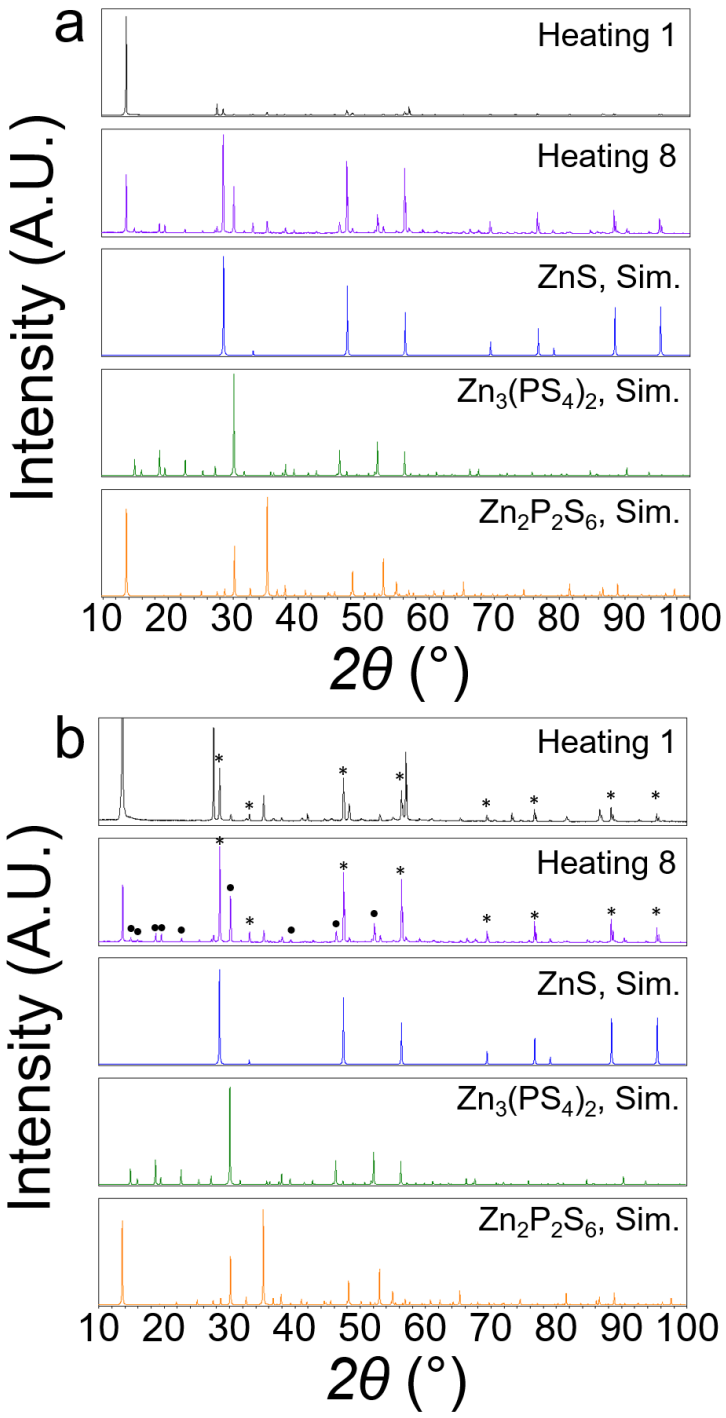

Figure S8. a.) Full range and b.) zoomed in PXRD patterns of $Zn_2P_2S_6$ made from **Heating 1**, **Heating 8** and the simulated patterns of ZnS, $Zn_3(PS_4)_2$ and $Zn_2P_2S_6$. The asterisks and closed circles corresponds to the peaks from ZnS and $Zn_3(PS_4)_2$, respectively .The discrepancy in peak intensity between the experimental and simulated PXRD patterns stems from preferred orientation, a common occurrence for layered materials.

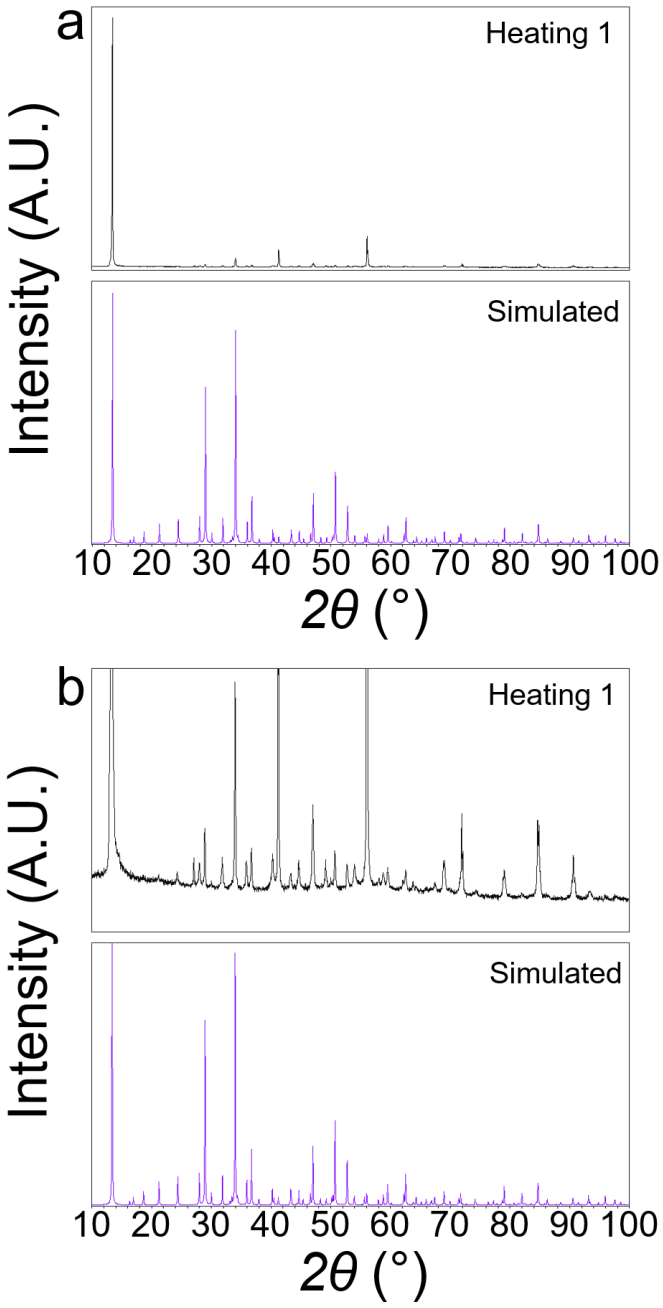

Figure S9. a.) Full range and b.) zoomed in PXRD patterns of $Cd_2P_2S_6$ made from **Heating 1** and the simulated pattern. The discrepancy in peak intensity between the experimental and simulated PXRD patterns stems from preferred orientation, a common occurrence for layered materials.

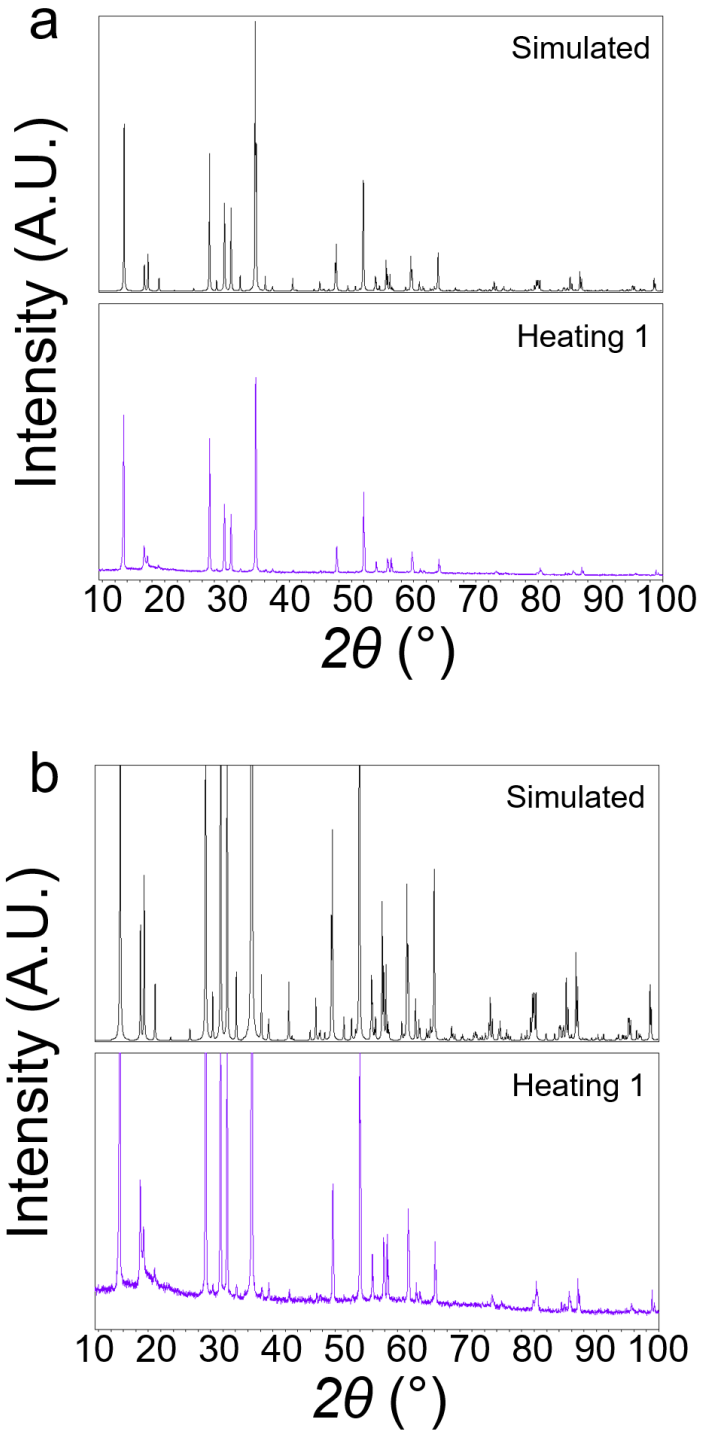

Figure S10. a.) Full range and b.) zoomed in PXRD patterns of $Mg_2P_2S_6$ made from **Heating 1** and the simulated pattern. The discrepancy in peak intensity between the experimental and simulated PXRD patterns stems from preferred orientation, a common occurrence for layered materials.

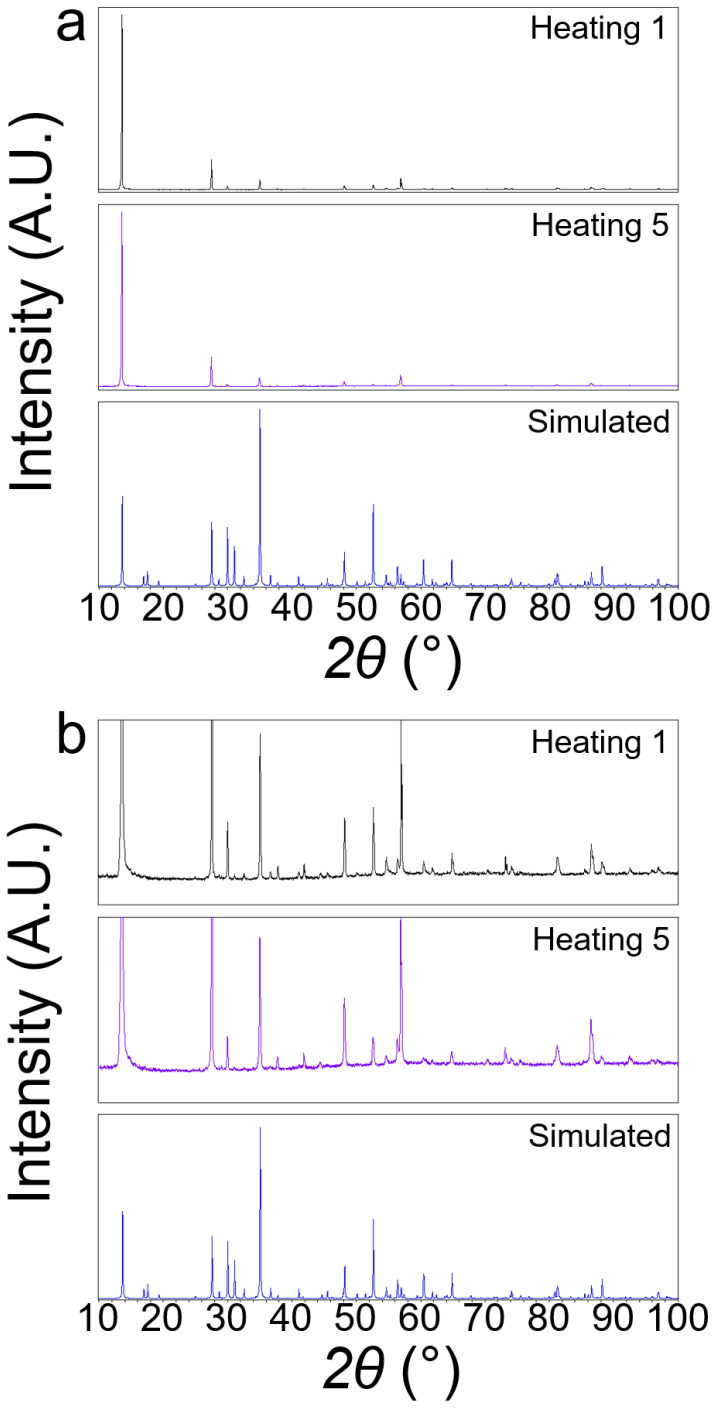

Figure S11. a.) Full range and b.) zoomed in PXRD patterns of $MnFeP_2S_6$ made from **Heating 1**, **Heating 5**, and the simulated pattern. The discrepancy in peak intensity between the experimental and simulated PXRD patterns stems from preferred orientation, a common occurrence for layered materials.

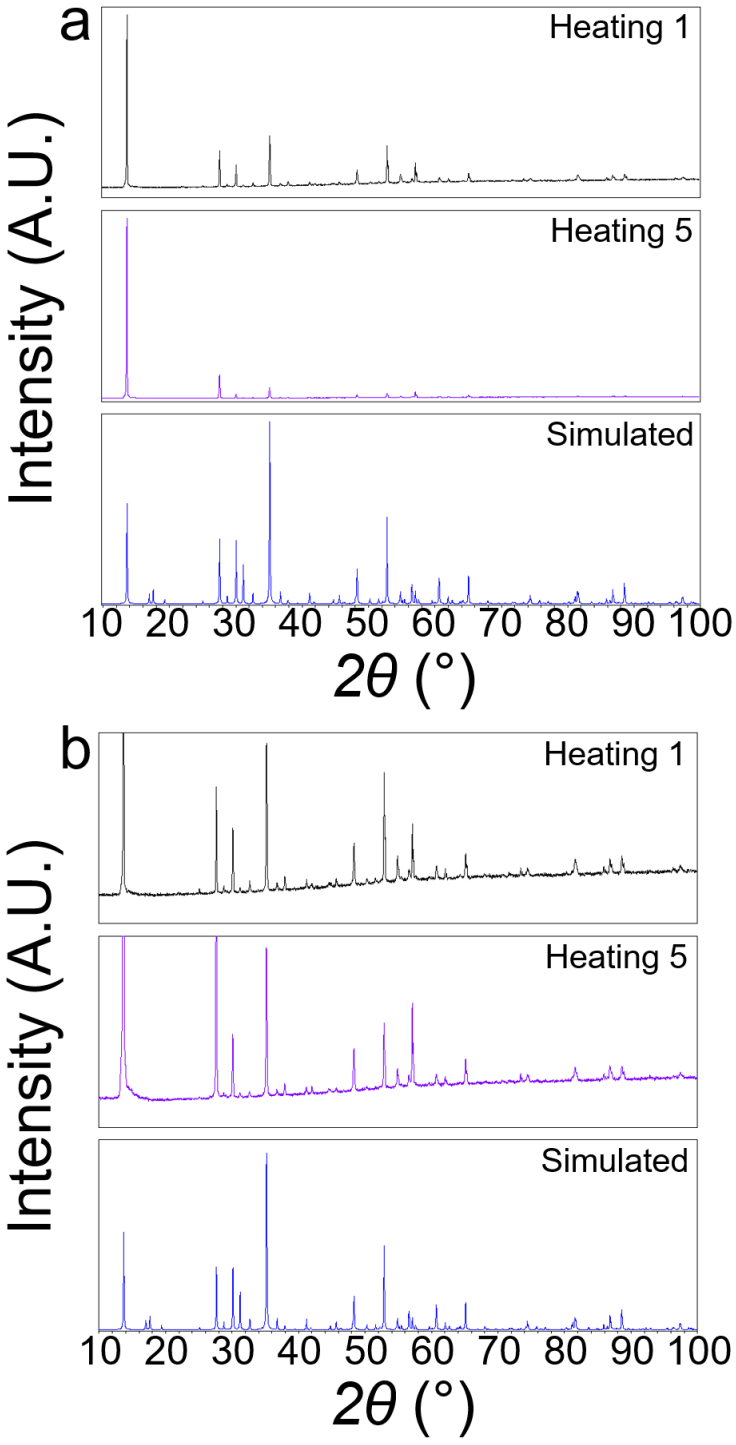

Figure S12. a.) Full range and b.) zoomed in PXRD patterns of $MnCoP_2S_6$ made from **Heating 1**, **Heating 5**, and the simulated pattern. The discrepancy in peak intensity between the experimental and simulated PXRD patterns stems from preferred orientation, a common occurrence for layered materials.

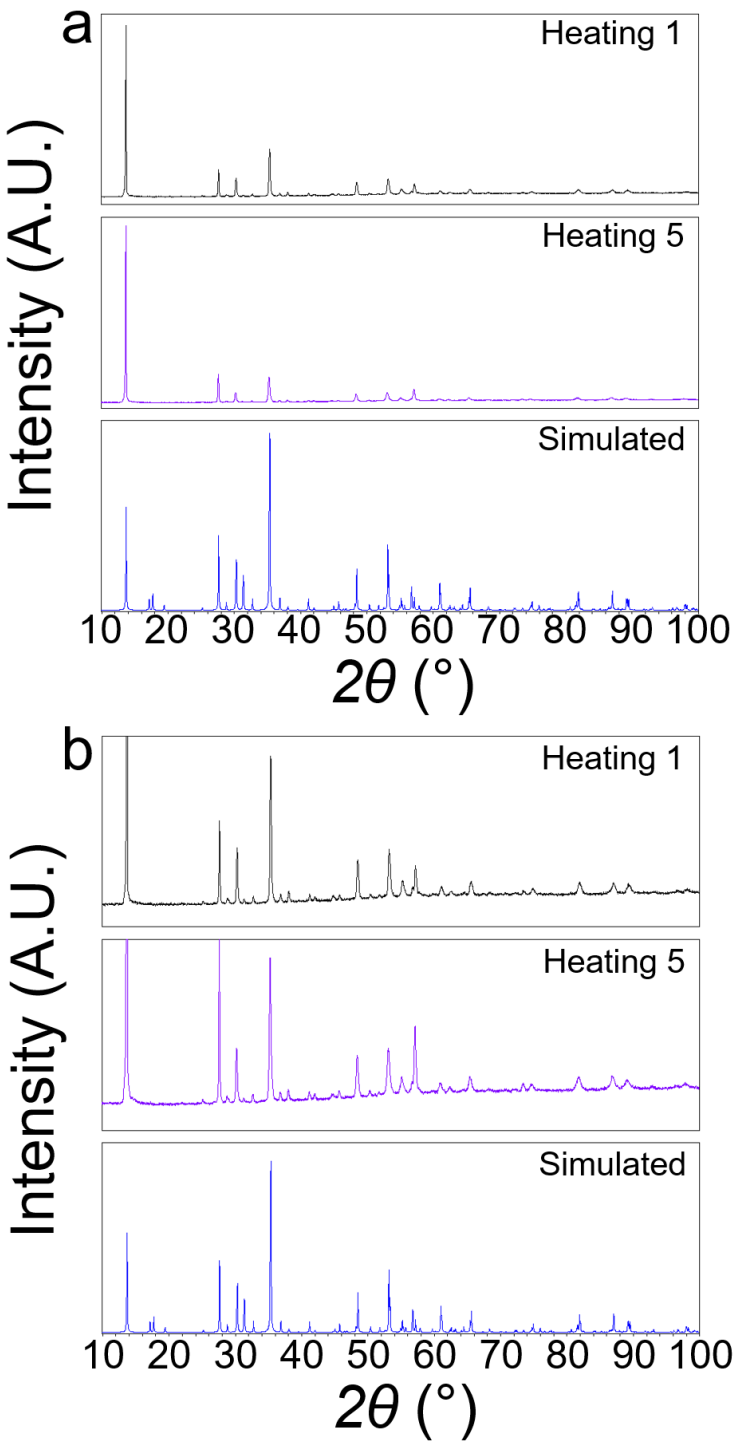

Figure S13. a.) Full range and b.) zoomed in PXRD patterns of $MnNiP_2S_6$ made from **Heating 1**, **Heating 5**, and the simulated pattern. The discrepancy in peak intensity between the experimental and simulated PXRD patterns stems from preferred orientation, a common occurrence for layered materials.

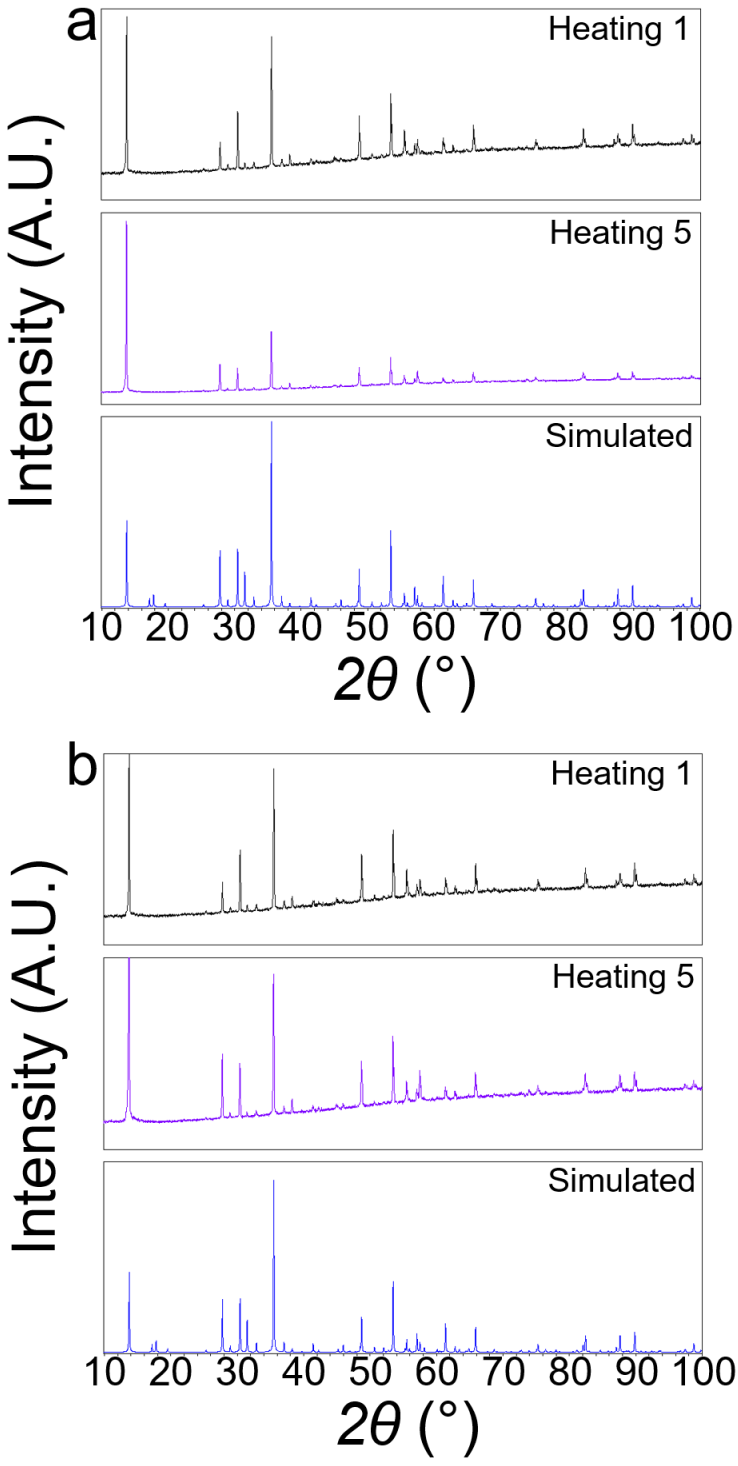

Figure S14. a.) Full range and b.) zoomed in PXRD patterns of $FeCoP_2S_6$ made from **Heating 1**, **Heating 5**, and the simulated pattern. The discrepancy in peak intensity between the experimental and simulated PXRD patterns stems from preferred orientation, a common occurrence for layered materials.

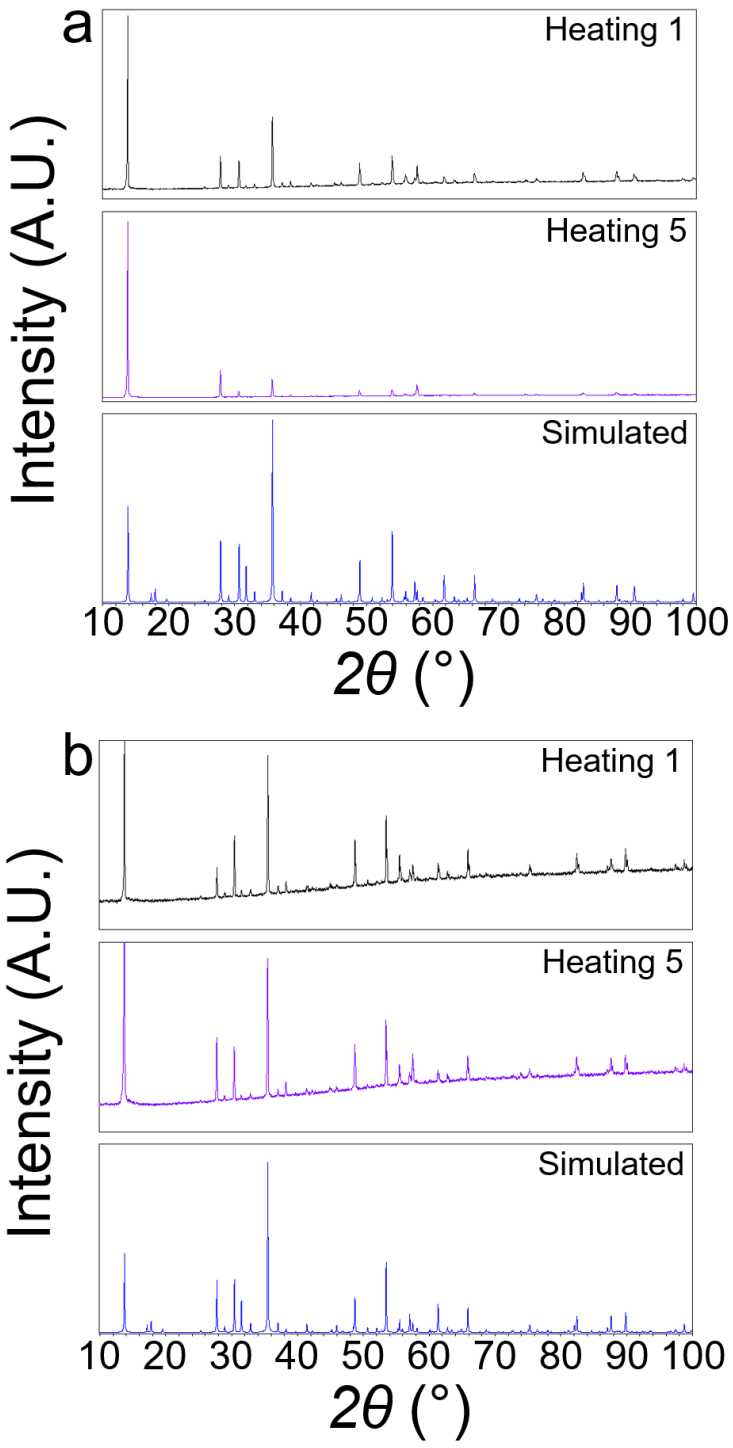

Figure S15. a.) Full range and b.) zoomed in PXRD patterns of $FeNiP_2S_6$ made from **Heating 1**, **Heating 5**, and the simulated pattern. The discrepancy in peak intensity between the experimental and simulated PXRD patterns stems from preferred orientation, a common occurrence for layered materials.

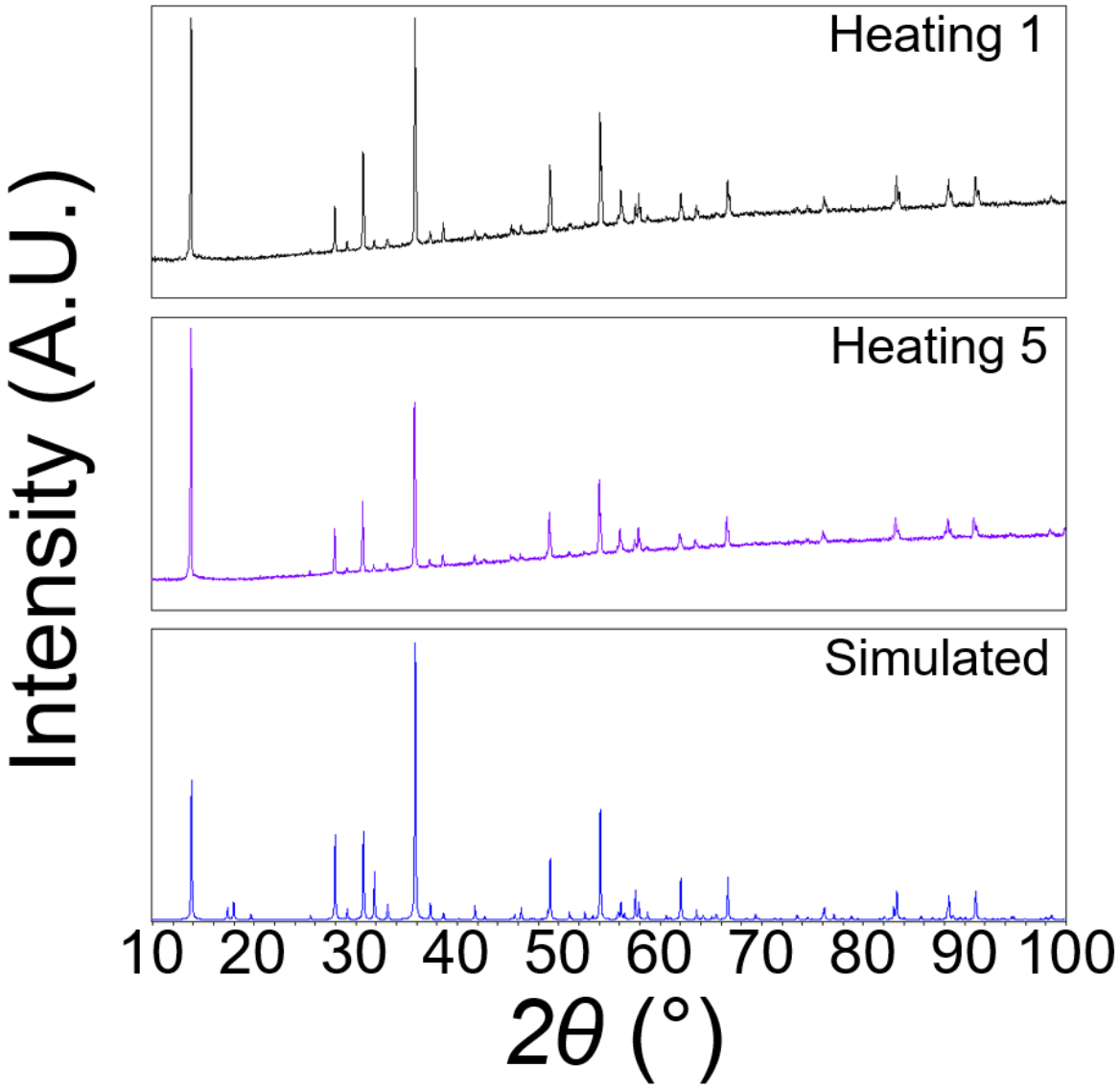

Figure S16. PXRD patterns of $CoNiP_2S_6$ made from **Heating 1**, **Heating 5**, and the simulated pattern. The discrepancy in peak intensity between the experimental and simulated PXRD patterns stems from preferred orientation, a common occurrence for layered materials.

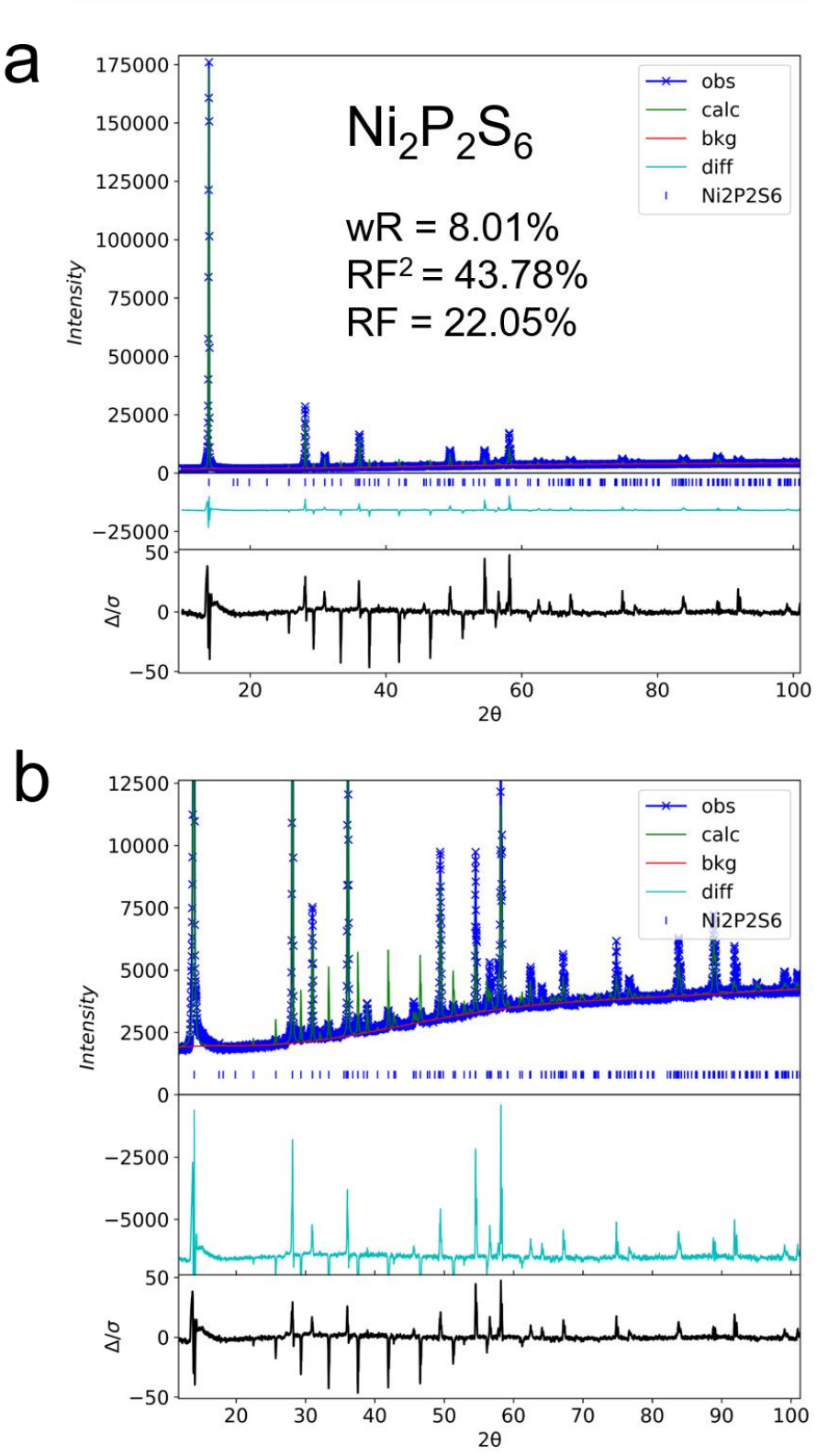

Figure S17. Experimental PXRD powder pattern for $Ni_2P_2S_6$ (**Heating 1**) with calculated and difference patterns from Rietveld refinement.

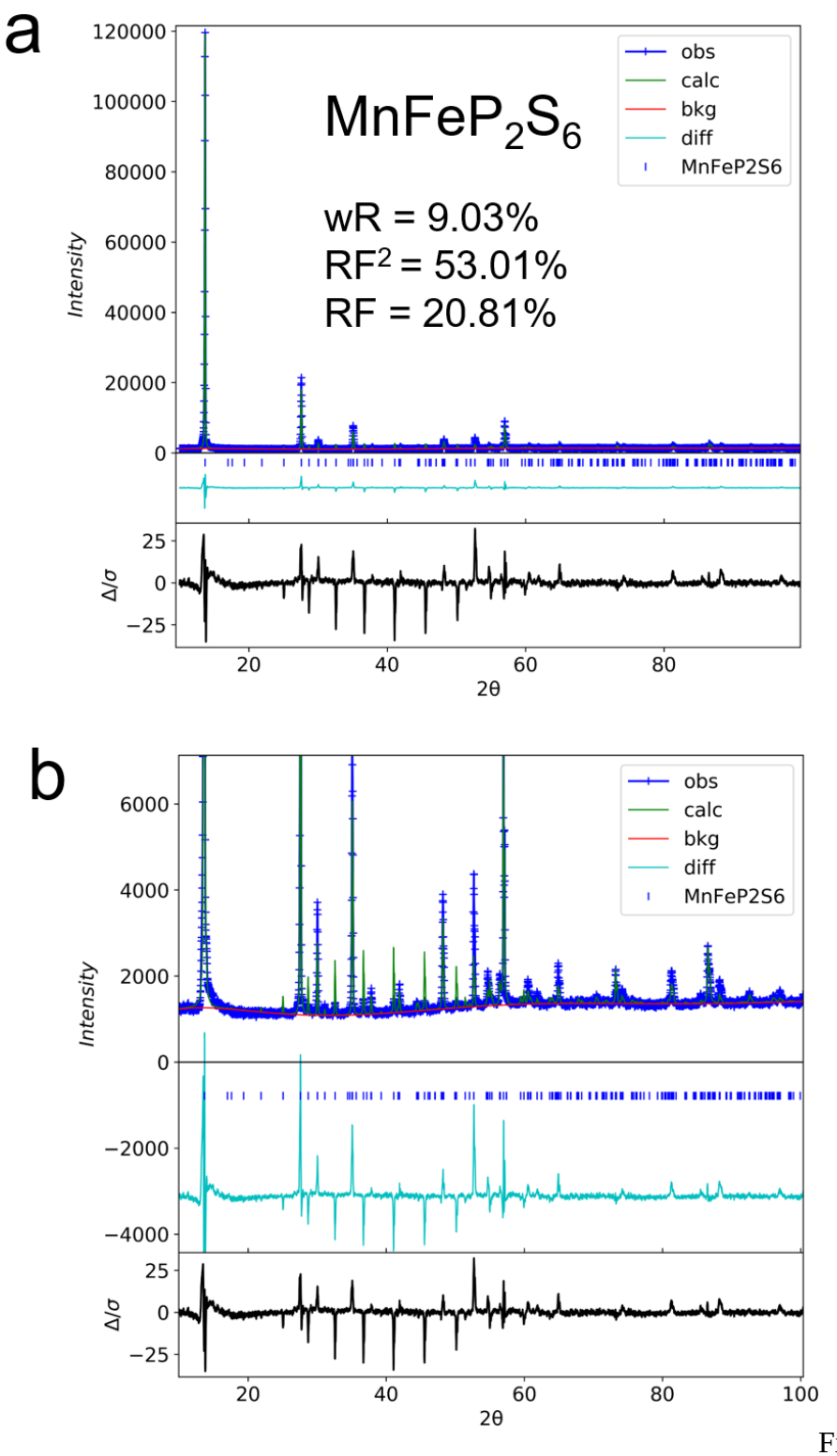

Figure S18. Experimental PXRD powder pattern for $MnFeP_2S_6$ (**Heating 1**) with calculated and difference patterns from Rietveld refinement.

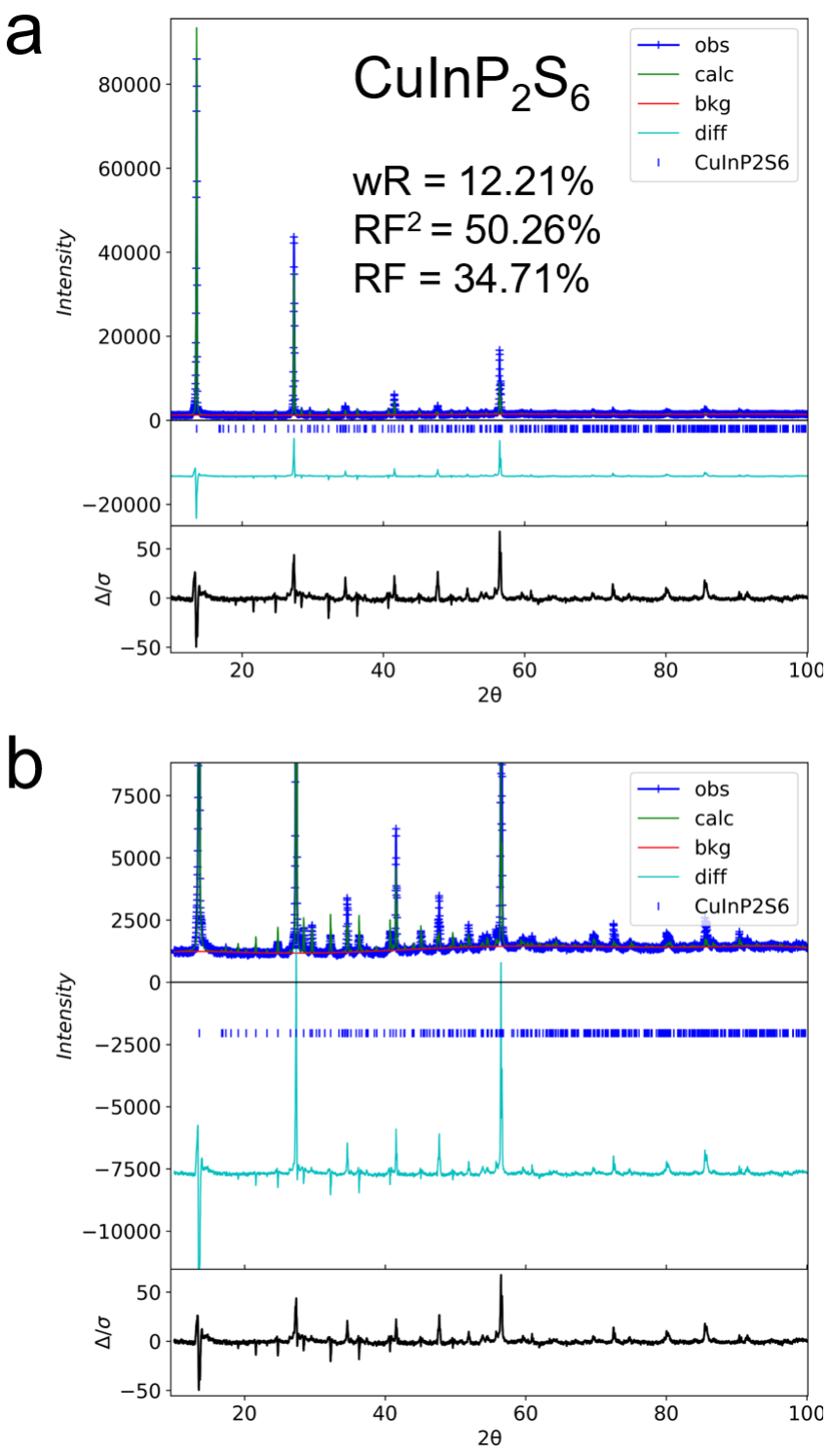

Figure S19. Experimental PXRD powder pattern for $CuInP_2S_6$ (**Heating 1**) with calculated and difference patterns from Rietveld refinement.

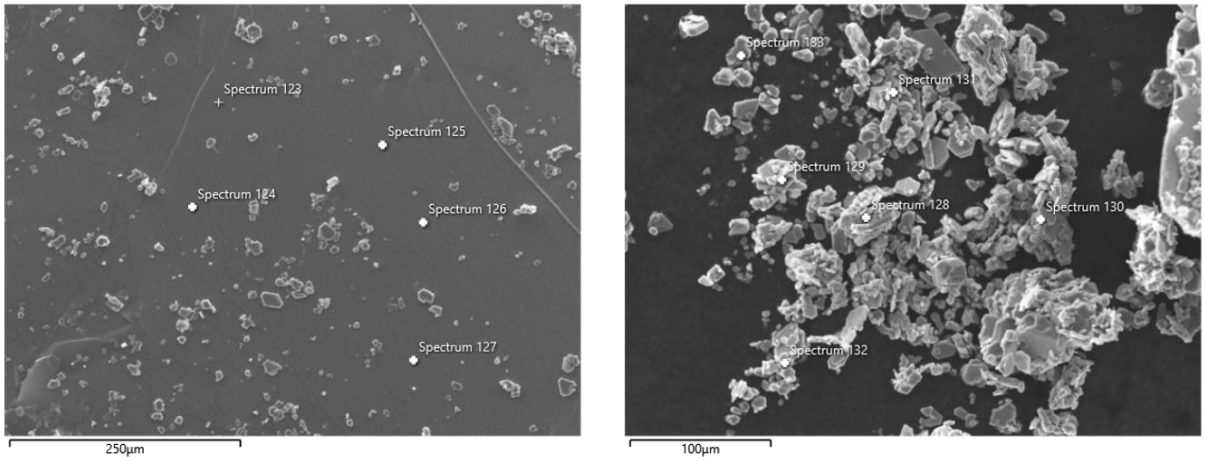

Figure S20. SEM images of $MnFeP_2S_6$ made from **Heating 5** (540°C).

Table S2. EDS values and statistics of $MnFeP_2S_6$ made from **Heating 5** (540°C).

Label	P at.%	S at.%	Mn at.%	Fe at.%
123	20.85	60.09	10.64	8.42
124	20.35	59.87	11	8.78
125	20.66	59.84	11	8.5
126	20.63	59.84	11.09	8.45
127	20.9	60.02	10.69	8.39
128	21.18	59.78	11.14	7.9
129	20.43	59.94	10.32	9.31
130	20.59	61.85	9.19	8.38
132	20.87	57.04	11.97	10.12
133	20.76	60.66	8.25	10.33

Statistic	P at.%	S at.%	Mn at.%	Fe at.%
Max	21.18	61.85	11.97	10.33
Min	20.35	57.04	8.25	7.9
Average	20.72	59.89	10.53	8.86
Standard Deviation	0.24	1.18	1.07	0.81

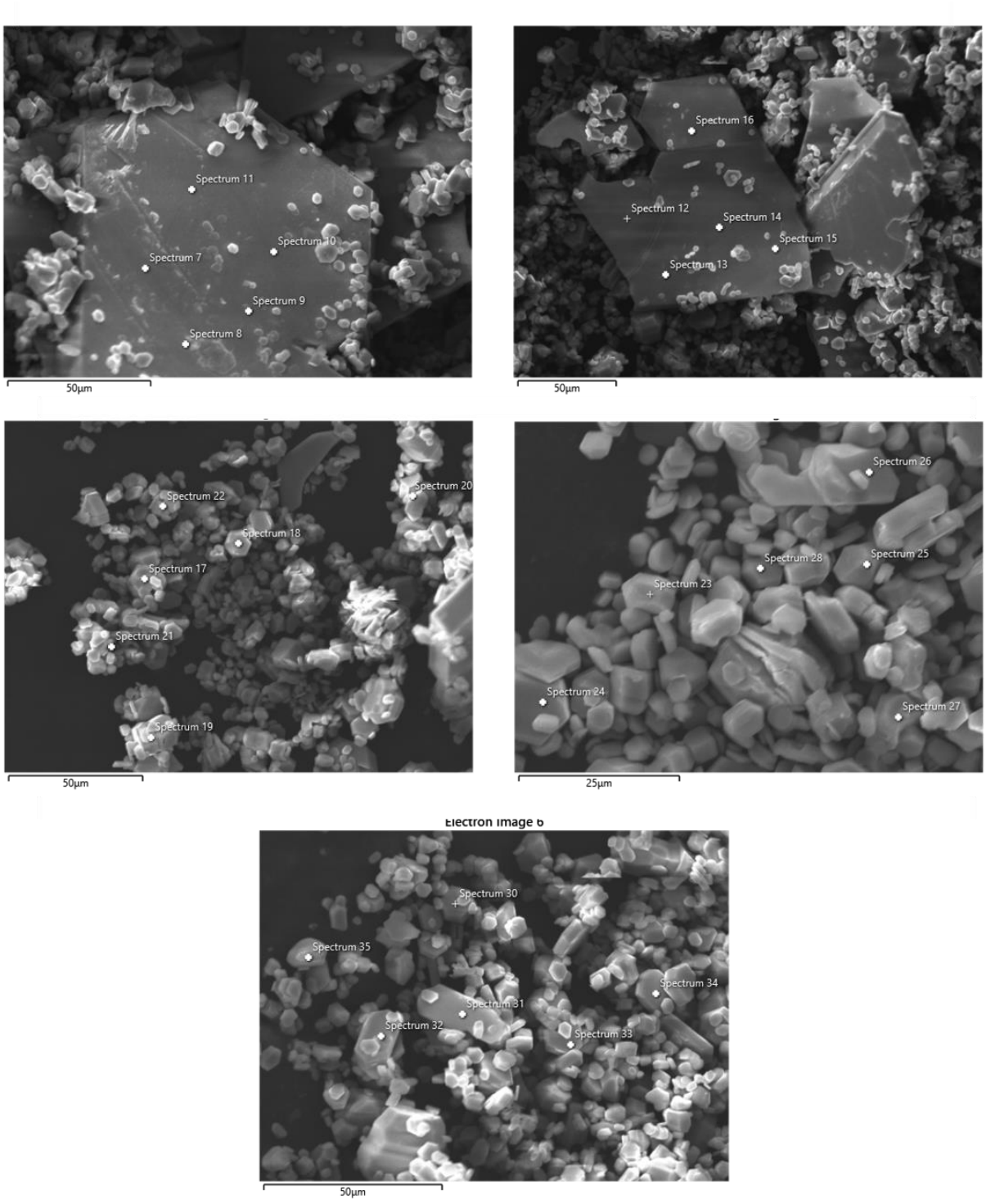

Figure S21. SEM images of $MnCoP_2S_6$ made from **Heating 5** (540°C).

Table S3. EDS values and statistics of $MnCoP_2S_6$ made from **Heating 5** (540°C).

Label	P at.%	S at.%	Mn at.%	Co at.%
7	20.43	58.05	10.68	10.85
8	20.55	57.52	10.76	11.18
9	20.67	57.99	10.63	10.71
10	20.34	58.91	10.38	10.37
11	20.36	58.38	10.39	10.87
12	20.92	59.33	10.69	9.06
13	20.56	59.24	10.7	9.51
14	20.48	59.68	10.38	9.46
15	20.56	60.82	10.03	8.59
16	20.46	59.42	10.79	9.33
18	20.83	60.5	9.45	9.22
19	20.7	59.85	10.54	8.91
20	21.27	58	10.66	10.06
22	20.76	60.12	9.73	9.39
23	20.56	60.89	11.65	6.9
24	20.82	59.54	9.72	9.92
25	21.04	60.26	9.38	9.32
27	20.46	58.87	10.6	10.07
28	20.63	61.03	9.06	9.28
30	20.68	58.08	10.91	10.33
31	20.54	60.97	9.13	9.36
32	20.79	60.04	9.9	9.26
33	20.63	60.09	10.7	8.58

Statistic	P at.%	S at.%	Mn at.%	Co at.%
Max	21.27	61.03	11.65	11.18
Min	20.34	57.52	9.06	6.9
Average	20.65	59.46	10.3	9.59
Standard Deviation	0.22	1.08	0.64	0.94

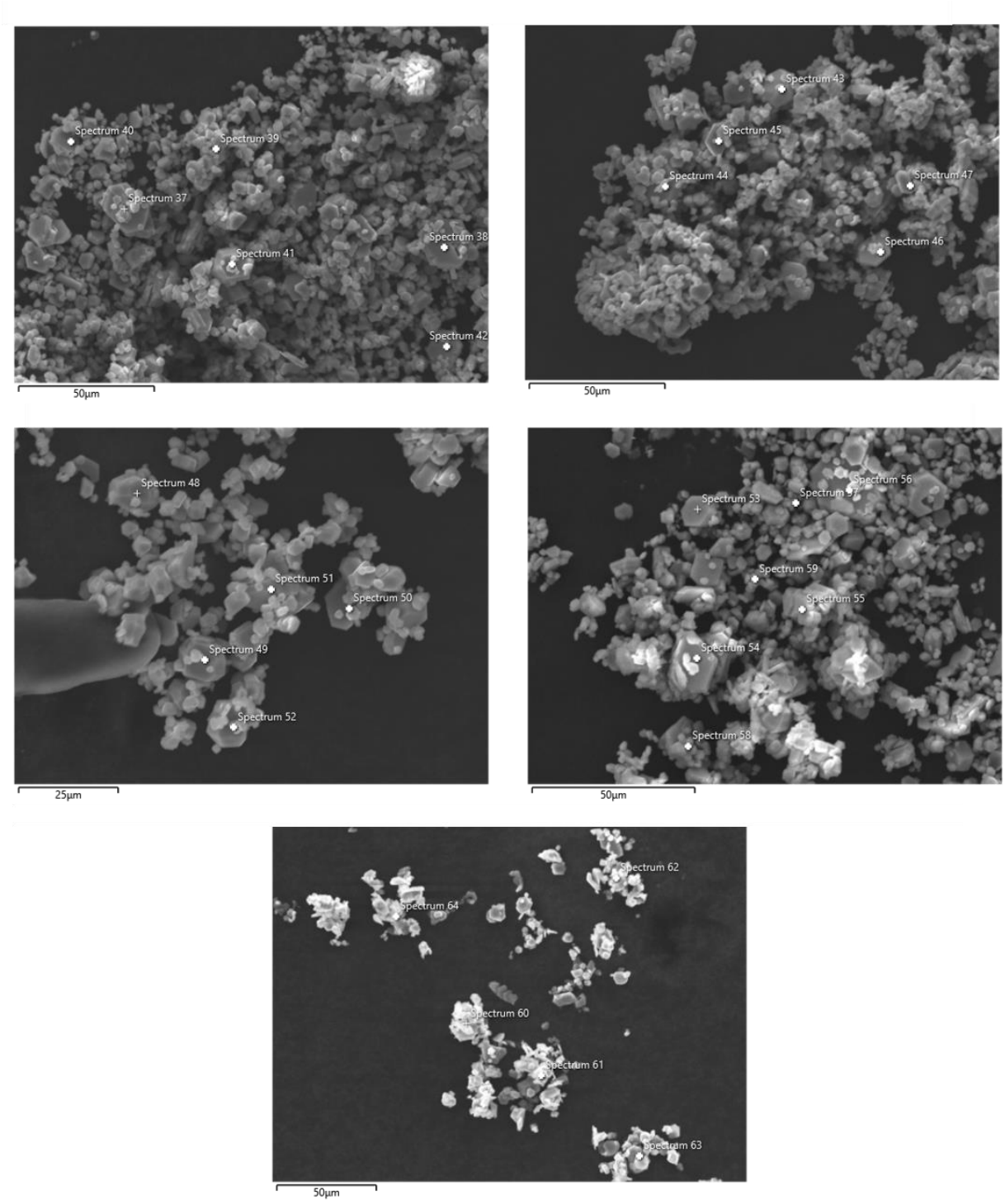

Figure S22. SEM images of $MnNiP_2S_6$ made from **Heating 5** (540°C).

Table S4. EDS values and statistics of $MnNiP_2S_6$ made from **Heating 5** (540°C).

Label	P at.%	S at.%	Mn at.%	Ni at.%
37	20.65	57.05	14.19	8.1
38	20.68	58.54	12.07	8.71
39	20.56	59.42	10.17	9.84
41	21	59.69	11.07	8.24
42	20.86	61.29	8.2	9.64
43	20.37	61.54	10.43	7.65
44	20.41	57.23	14.72	7.64
45	20.68	57.74	13.56	8.02
46	20.31	61.19	10.01	8.48
47	21.05	58.72	12.82	7.4
49	20.35	60.12	11.52	8.01
50	20.86	60.49	9.81	8.84
51	20.26	58.87	12.68	8.19
52	20.42	61.57	10.25	7.75
53	20.74	61.6	10.78	6.88
55	20.74	61.38	11.01	6.86
56	20.44	61.83	11.25	6.48
59	20.44	59.04	11.52	9
60	20.33	60.06	10.71	8.89
61	20.47	61.17	10.8	7.56
62	20.53	61.87	10.35	7.26
63	20.72	61.15	10.16	7.96
64	20.29	60.45	11.1	8.16

Statistic	P at.%	S at.%	Mn at.%	Ni at.%
Max	21.05	61.87	14.72	9.84
Min	20.26	57.05	8.2	6.48
Average	20.57	60.09	11.27	8.07
Standard Deviation	0.23	1.51	1.51	0.84

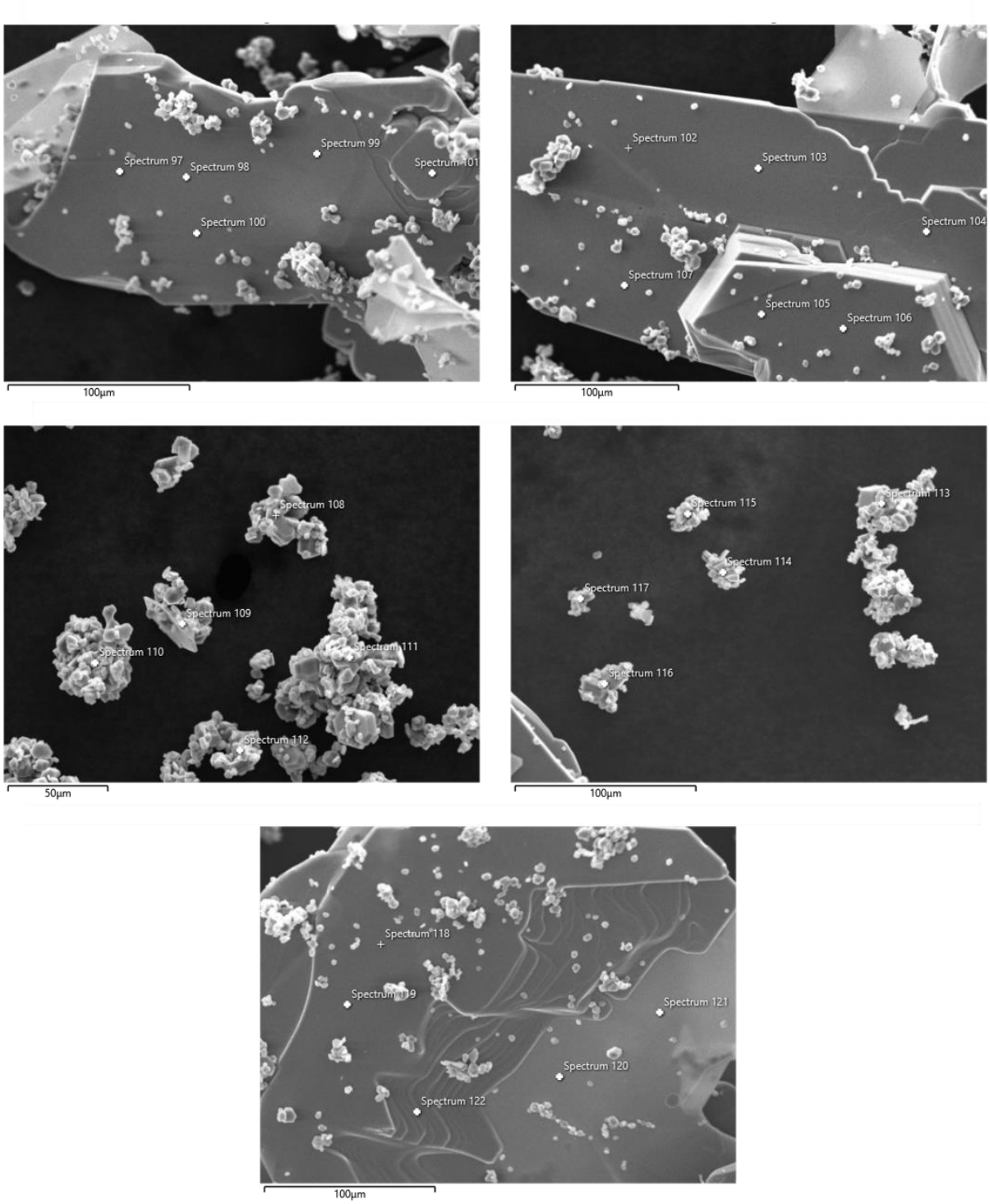

Figure S23. SEM images of $FeCoP_2S_6$ made from **Heating 5** (540°C).

Table S5. EDS values and statistics of $FeCoP_2S_6$ made from **Heating 5** (540°C).

Label	P at.%	S at.%	Fe at.%	Co at.%
97	20.71	60.6	5.83	12.86
98	20.72	60.66	5.74	12.88
99	20.55	60.74	4.91	13.8
100	20.77	60.19	5.74	13.3
101	20.94	60.42	5.73	12.91
102	20.83	61.21	5.17	12.79
103	20.68	61.15	5.03	13.14
104	20.86	60.93	5.31	12.9
105	20.47	61.04	5.47	13.02
106	20.66	60.83	5.45	13.05
107	20.53	61.16	5.05	13.26
108	20.77	58.11	11.22	9.9
109	21.17	58.95	9.94	9.94
110	20.59	59.89	9.94	9.57
111	20.06	57.63	11.34	10.97
112	20.63	59.75	10.32	9.3
113	20.6	58.38	10.57	10.45
114	20.87	61	8.7	9.42
115	21.17	61.08	8.11	9.64
117	20.74	58.33	10.22	10.72
118	20.57	58.66	5.05	15.72
119	20.43	58.71	4.83	16.03
120	20.35	59.19	4.84	15.61
121	20.43	59.15	4.98	15.45

Statistic	P at.%	S at.%	Fe at.%	Co at.%
Max	21.17	61.21	11.34	16.03
Min	20.06	57.63	4.83	9.3
Average	20.67	59.91	7.06	12.36
Standard Deviation	0.25	1.16	2.45	2.13

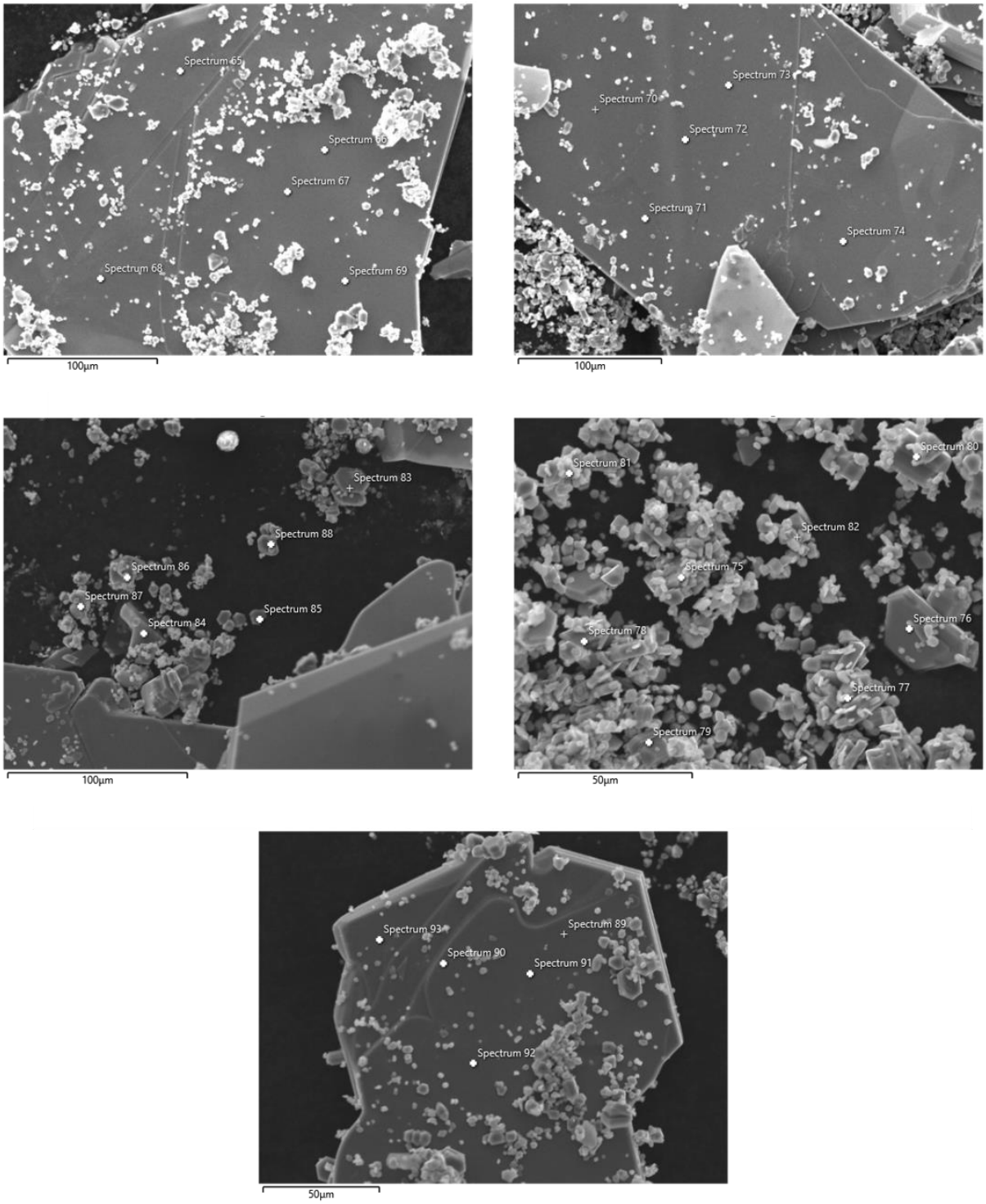

Figure S24. SEM images of $FeNiP_2S_6$ made from **Heating 5** (540°C).

Table S6. EDS values and statistics of $FeNiP_2S_6$ made from **Heating 5** (540°C).

Label	P at.%	S at.%	Fe at.%	Ni at.%
65	20.7	60.31	9.87	9.12
66	20.64	60.26	9.98	9.12
67	20.45	60.64	9.99	8.92
68	20.79	59.89	9.95	9.37
69	20.57	60.89	9.61	8.93
70	20.65	59.05	10.57	9.73
71	20.82	59.36	10.53	9.28
72	20.39	60.53	10.29	8.79
73	20.76	60.73	9.84	8.66
74	20.84	60.72	9.81	8.63
75	20.91	59.97	10.16	8.97
76	20.67	61.09	9.84	8.4
77	20.91	60.1	10.03	8.96
80	20.73	61.57	9.34	8.36
83	20.46	60.85	9.36	9.32
84	20.81	61.01	9.76	8.42
85	20.19	59.26	11.5	9.05
86	20.76	57.91	12.01	9.32
87	20.52	61.38	10.12	7.97
88	20.54	60.37	10.01	9.08
89	20.77	59.01	10.78	9.44
90	20.47	59.21	10.68	9.64
91	20.35	58.93	10.82	9.9
92	20.66	58.45	11.08	9.81
93	20.29	59.69	10.5	9.52

Statistic	P at.%	S at.%	Fe at.%	Ni at.%
Max	20.91	61.57	12.01	9.9
Min	20.19	57.91	9.34	7.97
Average	20.63	60.05	10.26	9.07
Standard Deviation	0.2	0.95	0.64	0.49

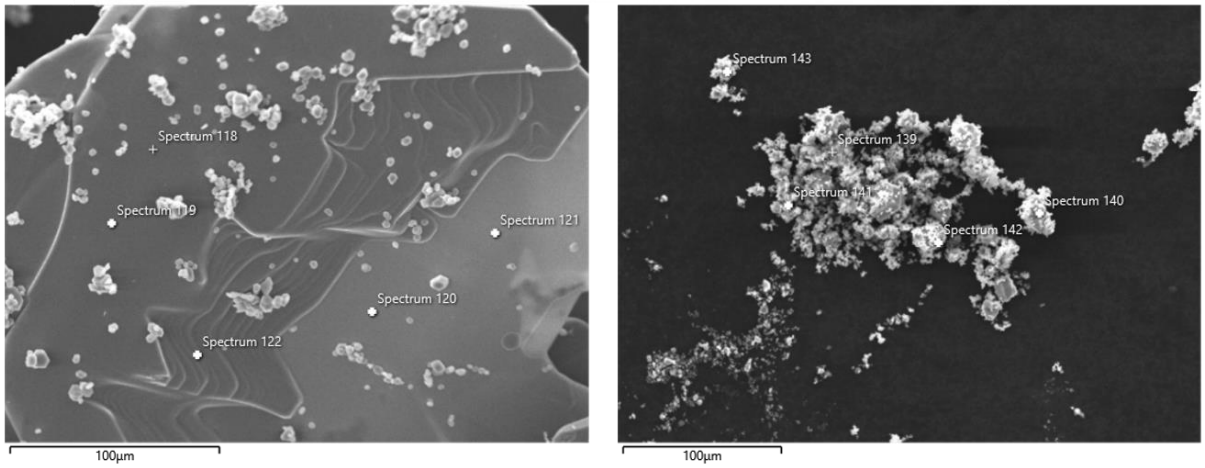

Figure S25. SEM images of $CoNiP_2S_6$ made from **Heating 5** (540°C).

Table S7. EDS values and statistics of $CoNiP_2S_6$ made from **Heating 5** (540°C).

Label	P at.%	S at.%	Co at.%	Ni at.%
134	20.95	60.2	13.16	5.69
135	20.44	59.99	14.41	5.16
136	20.92	60.6	12.98	5.5
137	20.71	60.18	13.85	5.26
138	20.79	61.1	11.49	6.62
139	21.03	61.66	7.76	9.55
140	19.98	58.16	12.03	9.82
141	20.62	61.08	10.49	7.81
142	20.49	59.7	10.94	8.86
143	20.6	61	12.61	5.79

Statistic	P at.%	S at.%	Co at.%	Ni at.%
Max	21.03	61.66	14.41	9.82
Min	19.98	58.16	7.76	5.16
Average	20.66	60.38	11.96	7
Standard Deviation	0.31	0.98	1.93	1.84

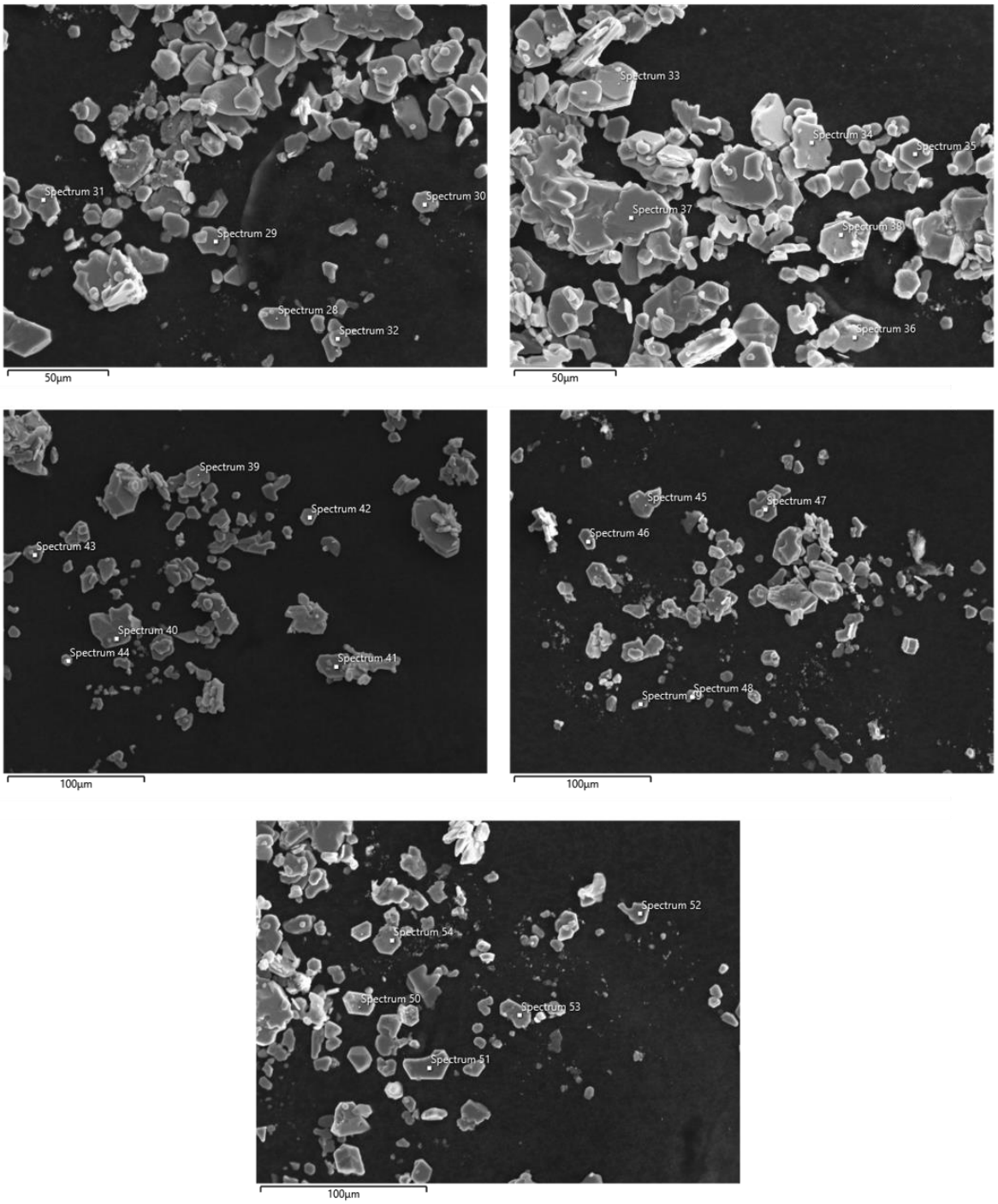

Figure S26. SEM images of $MnFeP_2S_6$ made from **Heating 1** (650°C).

Table S8. EDS values and statistics of $MnFeP_2S_6$ made from **Heating 1** (650°C).

Label	P at.%	S at.%	Mn at.%	Fe at.%
28	20.35	59.76	9.76	10.13
29	20.63	59.77	10.16	9.44
30	20.18	61.05	9.27	9.5
31	20.73	57.88	10.51	10.89
32	20.65	60.16	10.11	9.09
33	20.48	61.69	9.33	8.49
34	20.58	60.92	7.67	10.83
35	20.61	59.34	9.46	10.59
36	20.21	52.98	11.85	14.96
37	20.84	60.15	9.02	9.98
38	20.49	61.16	9.55	8.8
39	20.82	60.96	8.97	9.25
40	20.62	60.19	10.36	8.83
41	20.77	60.33	9.78	9.12
42	20.55	61.43	8.23	9.79
43	20.49	57.23	12.86	9.42
44	20.63	60.89	8.93	9.56
45	20.55	61.29	7.99	10.17
46	20.93	57.05	11.28	10.74
47	21	59.07	9.74	10.18
48	20.72	59.58	12.42	7.28
49	20.08	61.26	8.28	10.38
50	20.62	58.77	10.47	10.14
51	20.63	59.21	9.89	10.28
52	20.73	60.12	8.99	10.16
53	20.12	60.95	9.8	9.14
54	20.73	59.57	10.98	8.72

Statistic	P at.%	S at.%	Mn at.%	Fe at.%
Max	21	61.69	12.86	14.96
Min	20.08	52.98	7.67	7.28
Average	20.58	59.73	9.84	9.85
Standard Deviation	0.23	1.82	1.26	1.31

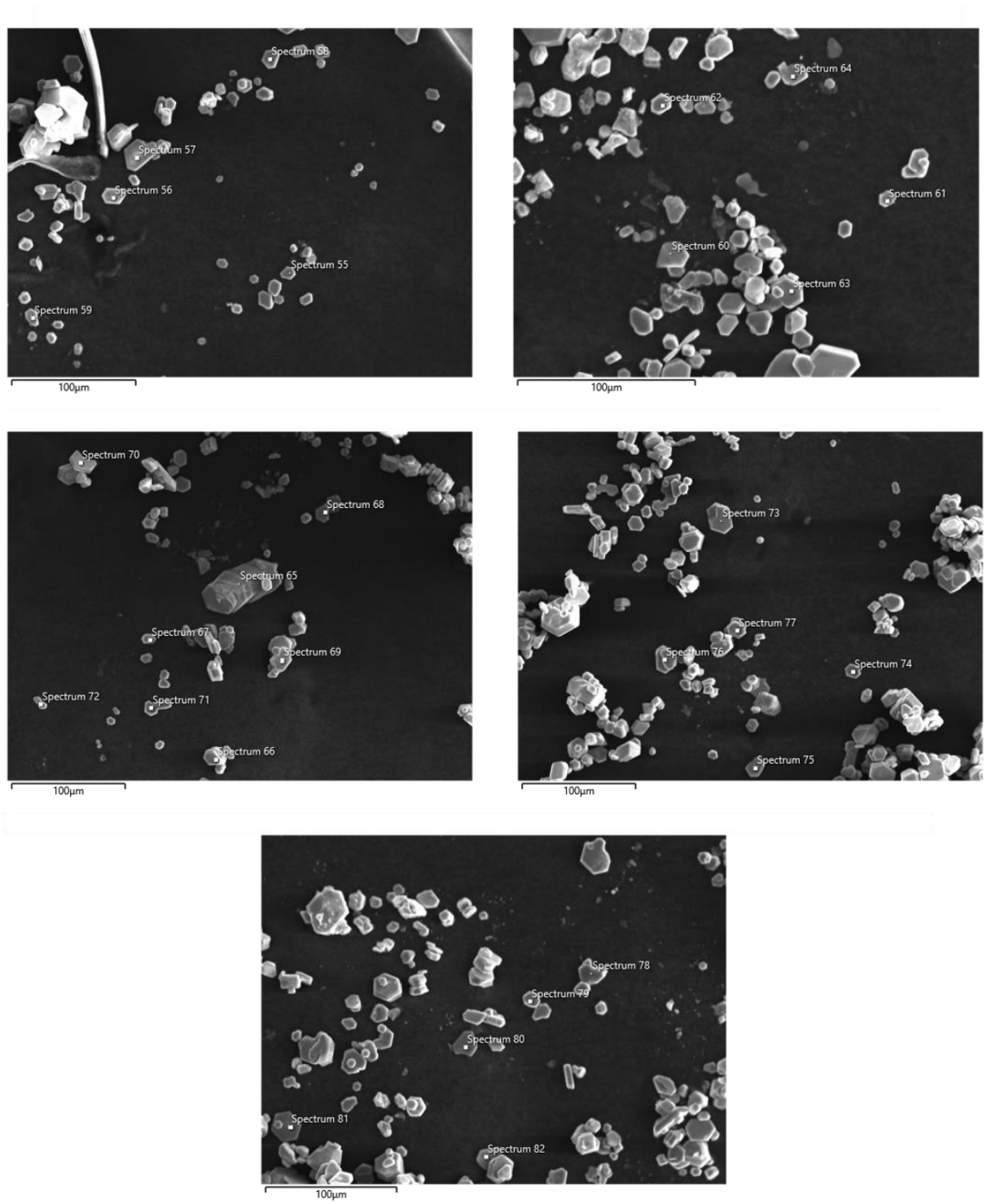

Figure S27. SEM images of $MnCoP_2S_6$ made from **Heating 1** (650°C).

Table S9. EDS values and statistics of $MnCoP_2S_6$ made from **Heating 1** (650°C).

Label	P at.%	S at.%	Mn at.%	Co at.%
55	21.08	59.82	10.03	9.06
56	20.54	60.25	9.67	9.54
57	20.54	60.42	10.24	8.8
58	20.67	60.04	11.2	8.09
59	20.66	59.99	9.38	9.97
60	20.62	61.64	9.01	8.72
61	20.52	61	9.31	9.17
62	20.4	60.56	9.69	9.35
63	20.79	58.78	10.5	9.93
64	20.83	60.42	10.37	8.37
65	20.72	60.64	9.36	9.28
66	20.75	53.57	13.02	12.66
67	20.88	59.71	10.14	9.27
68	20.49	56.42	11.83	11.26
69	20.2	54.39	12.89	12.52
70	20.58	61.8	9.05	8.57
71	20.74	60.32	10.02	8.92
72	21.47	60.35	9.13	9.05
73	20.88	59.73	10.96	8.43
74	20.63	60	9.97	9.41
75	20.94	60.55	9.57	8.93
76	20.61	60.53	9.65	9.2
77	20.69	58.33	11.02	9.97
78	20.43	59.45	10.13	9.98
79	20.35	61.17	10.69	7.79
80	20.69	60.07	10.29	8.95
81	20.51	59.72	10.08	9.69
82	20.59	59.43	10.16	9.81

Statistic	P at.%	S at.%	Mn at.%	Co at.%
Max	21.47	61.8	13.02	12.66
Min	20.2	53.57	9.01	7.79
Average	20.67	59.61	10.26	9.45
Standard Deviation	0.24	1.89	1.01	1.12

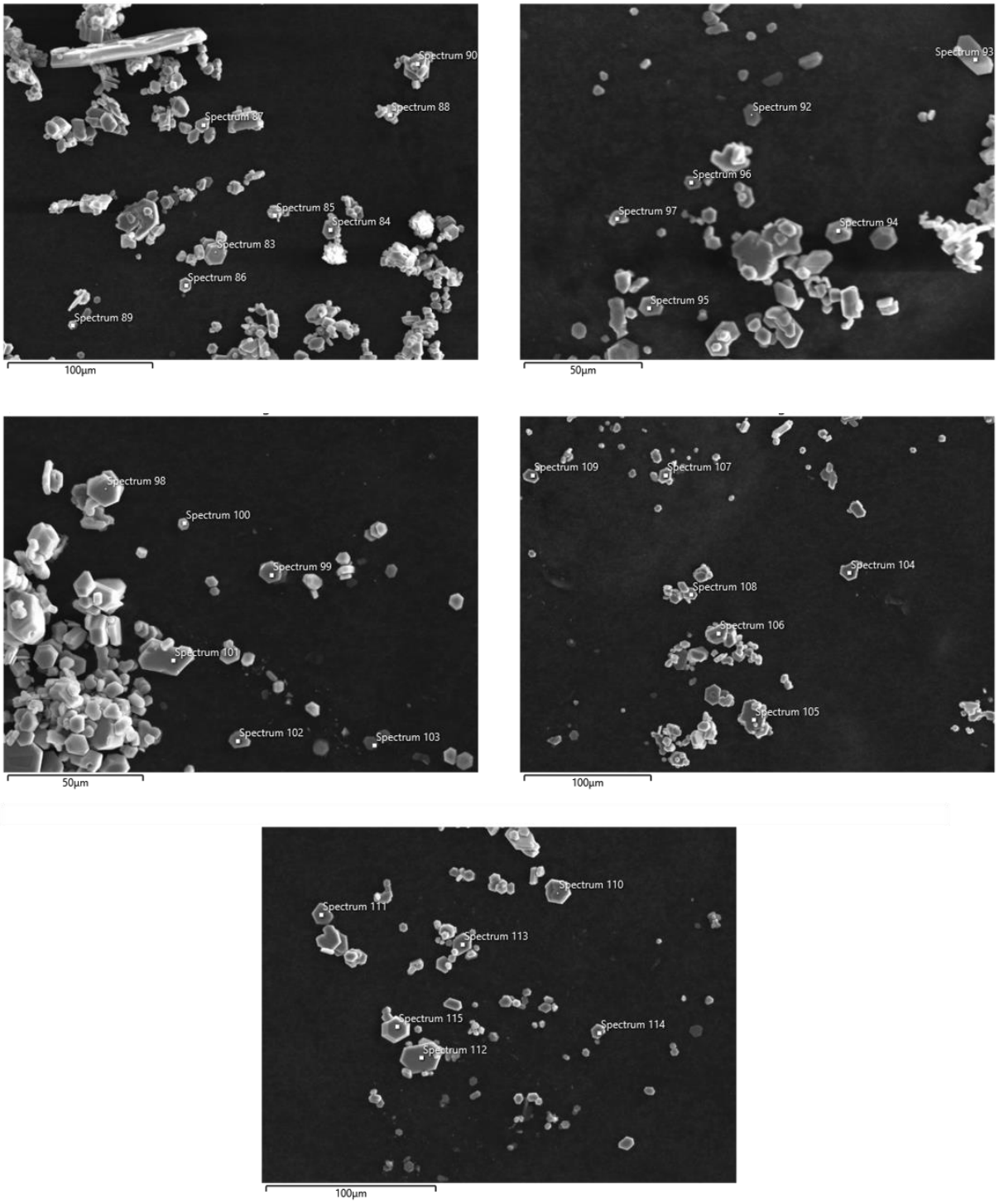

Figure S28. SEM images of $MnNiP_2S_6$ made from **Heating 1** (650°C).

Table S10. EDS values and statistics of $MnNiP_2S_6$ made from **Heating 1** (650°C).

Label	P at.%	S at.%	Mn at.%	Ni at.%
83	20.47	59.28	8.45	11.8
86	20.71	60.91	10.03	8.35
88	21	60.07	10.02	8.92
89	20.66	60.03	10.34	8.97
90	20.88	60.58	9.79	8.75
92	20.31	60.77	11.56	7.35
93	20.08	61.24	10.75	7.93
94	20.25	61.47	9.72	8.56
96	20.11	59.99	9.79	10.12
97	20.32	59.56	9.19	10.93
98	21.12	59.41	10.11	9.35
99	20.83	58.89	11.37	8.92
100	20.32	61.44	8.89	9.35
102	20.64	59.81	9.48	10.07
104	21.08	59.18	11.96	7.78
106	20.55	61.04	10.56	7.85
107	20.83	60.9	10.88	7.39
108	20.68	60.96	9.66	8.69
109	20.86	61.22	10.43	7.5
110	20.82	60.13	10.85	8.2
111	20.69	59.3	10.31	9.7
112	20.51	55.76	11.04	12.68
113	20.66	60.14	9.19	10.01
114	20.47	60.51	9.78	9.24
115	21.05	60.01	8.73	10.21

Statistic	P at.%	S at.%	Mn at.%	Ni at.%
Max	21.12	61.47	11.96	12.68
Min	20.08	55.76	8.45	7.35
Average	20.64	60.1	10.12	9.14
Standard Deviation	0.29	1.18	0.89	1.34

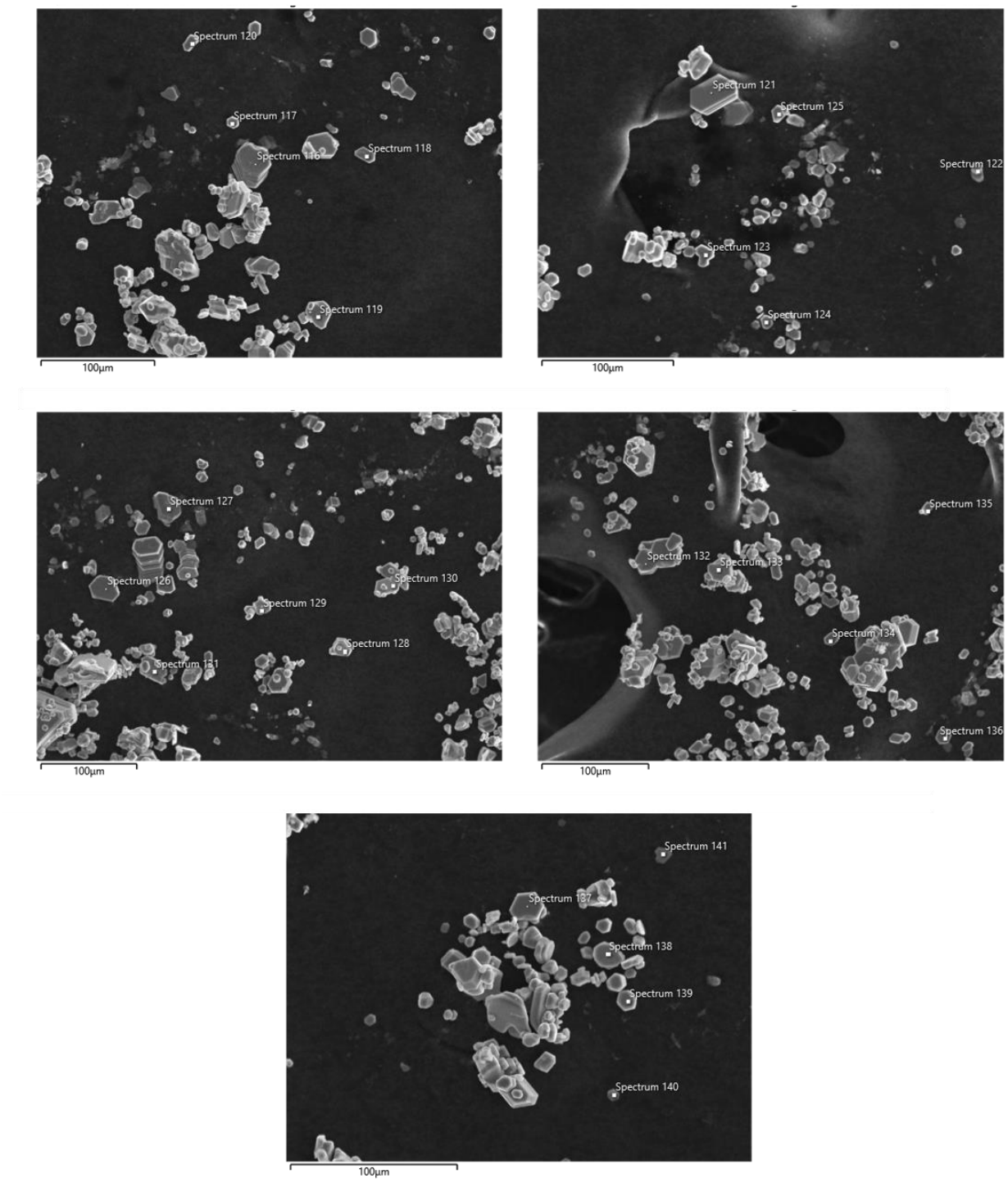

Figure S29. SEM images of $FeCoP_2S_6$ made from **Heating 1** (650°C).

Table S11. EDS values and statistics of $FeCoP_2S_6$ made from **Heating 1** (650°C).

Label	P at.%	S at.%	Fe at.%	Co at.%
116	20.75	60.74	10.15	8.36
117	20.33	59.92	12.73	7.02
118	20.99	61.55	8.93	8.53
119	20.69	61.29	9.07	8.94
120	20.8	58.96	13.33	6.91
121	20.62	58.63	10.76	9.98
122	20.86	60	9.58	9.57
123	21.52	60.51	8.97	9
124	20.37	60.49	9.72	9.42
125	20.9	60.27	11.41	7.42
126	20.67	58.8	11.52	9.01
127	20.87	60.32	9.48	9.34
128	19.65	46.91	17.68	15.76
129	19.21	46.41	17.79	16.59
130	20.97	61.4	9.47	8.16
131	20.66	60.56	9.85	8.92
132	20.82	59.3	10.68	9.2
133	20.58	60.84	9.93	8.65
134	20.72	59.05	10.14	10.09
135	20.62	59.79	9.78	9.81
136	20.71	59.62	11.04	8.63
137	20.81	60.54	9.93	8.73
138	21.09	60.41	9.84	8.66
139	20.82	60.1	9.94	9.14
140	20.51	60	10.01	9.48
141	20.28	59.82	10.47	9.43

Statistic	P at.%	S at.%	Fe at.%	Co at.%
Max	21.52	61.55	17.79	16.59
Min	19.21	46.41	8.93	6.91
Average	20.65	59.09	10.85	9.41
Standard Deviation	0.44	3.74	2.28	2.15

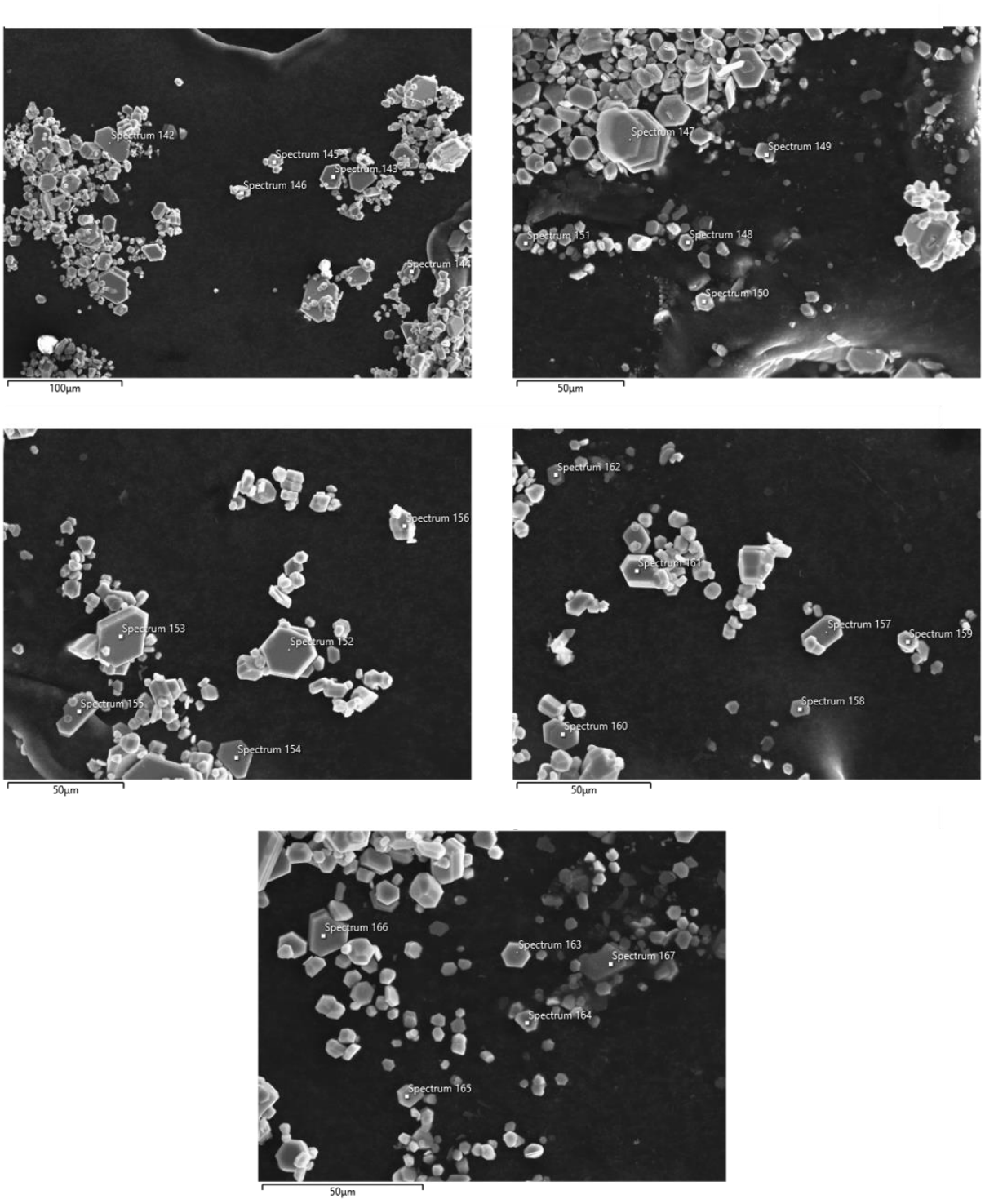

Figure S30. SEM images of $FeNiP_2S_6$ made from **Heating 1** (650°C).

Table S12. EDS values and statistics of $FeNiP_2S_6$ made from **Heating 1** (650°C).

Label	P at.%	S at.%	Fe at.%	Ni at.%
142	20.61	60.39	9.5	9.5
143	20.54	60.12	11.09	8.25
144	20.73	60.5	10.54	8.22
145	20.32	60	9.89	9.79
146	20.76	60.85	9.09	9.29
147	20.92	60.65	10.35	8.07
148	20.54	60.6	9.81	9.05
149	20.95	61.59	8.18	9.29
150	20.77	62.02	7.99	9.22
151	20.91	59.49	10.2	9.4
152	20.85	60.54	9.9	8.71
153	20.14	58.17	9.22	12.47
154	20.71	60.4	10.28	8.6
155	20.33	58.97	10.52	10.19
156	20.99	61	9.76	8.25
157	21.17	60.85	9.32	8.66
158	19.93	61.27	10.62	8.18
159	20.9	61.29	9.98	7.84
160	20.8	54.11	13.34	11.74
161	20.81	60.06	10.33	8.8
162	20.4	59.98	9.93	9.69
163	20.56	60.45	8.53	10.46
164	20.84	60.35	8.78	10.02
165	21.17	60.15	9.32	9.36
166	21.25	59.69	10.44	8.62
167	20.8	61.15	9.75	8.29

Statistic	P at.%	S at.%	Fe at.%	Ni at.%
Max	21.25	62.02	13.34	12.47
Min	19.93	54.11	7.99	7.84
Average	20.72	60.18	9.87	9.23
Standard Deviation	0.31	1.47	1.04	1.1

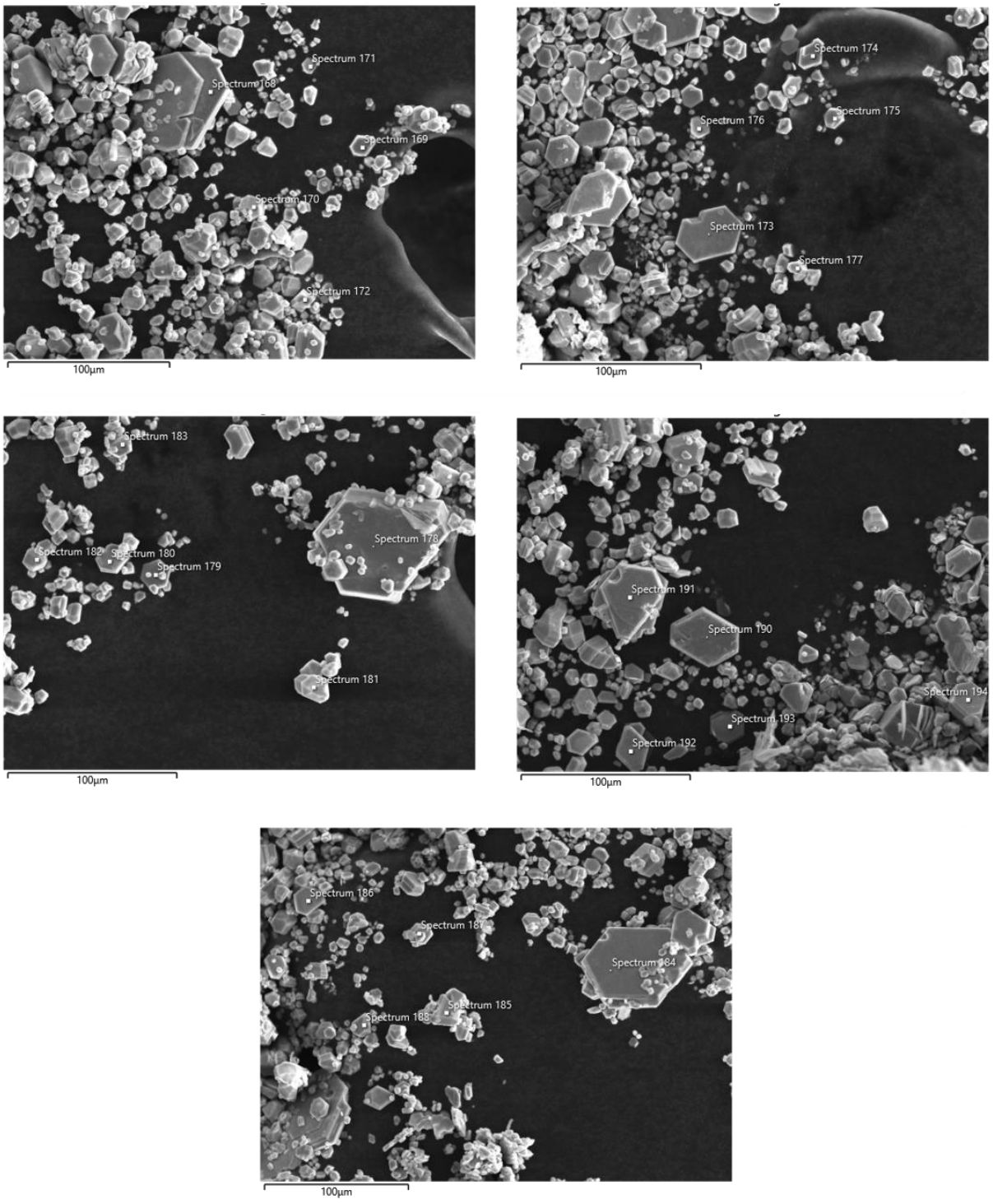

Figure S31. SEM images of $CoNiP_2S_6$ made from **Heating 1** (650°C).

Table S13. EDS values and statistics of $CoNiP_2S_6$ made from **Heating 1** (650°C).

Label	P at.%	S at.%	Co at.%	Ni at.%
168	20.64	59.71	10.77	8.88
169	21	60.06	9.52	9.42
170	20.57	62.25	7.77	9.42
171	20.77	61.95	8.03	9.25
172	20.91	60.98	7.62	10.49
173	20.55	60.41	9.08	9.96
174	20.73	60.71	8.73	9.83
175	20.72	59.9	9.21	10.17
176	20.9	61.69	8.5	8.92
177	20.51	62.11	8.25	9.13
178	20.72	56.02	10.54	12.72
179	20.3	59.64	9.13	10.93
180	20.64	61.79	8.46	9.11
181	20.59	61.46	8.44	9.51
182	20.9	59.17	9.03	10.9
183	20.51	60.26	8.68	10.55
184	20.86	61.23	7.52	10.39
185	20.61	62.69	6.55	10.14
186	21.15	61.67	8.77	8.41
187	20.46	61.99	6.17	11.39
188	20.92	60.96	8.42	9.71
190	20.7	60.36	10.13	8.81
191	20.68	60.41	9.27	9.64
192	20.48	60.31	8.87	10.34
193	20.99	59.83	9.07	10.11
194	21.13	61.62	8.84	8.4

Statistic	P at.%	S at.%	Co at.%	Ni at.%
Max	21.15	62.69	10.77	12.72
Min	20.3	56.02	6.17	8.4
Average	20.73	60.74	8.67	9.87
Standard Deviation	0.22	1.34	1.04	0.97

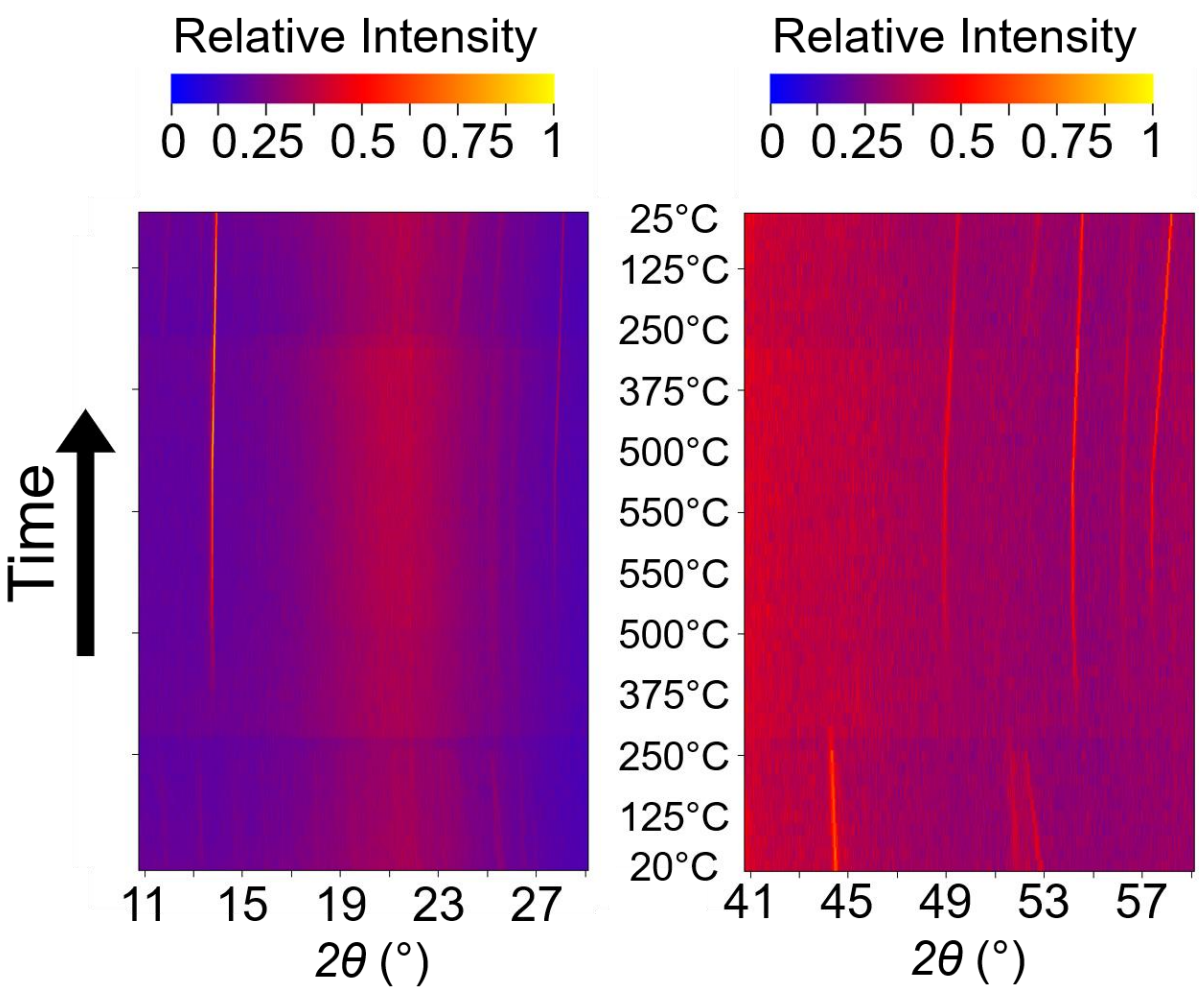

Figure S32. Full range VT-PXRD pattern from the Ni/P_2S_5 reaction.

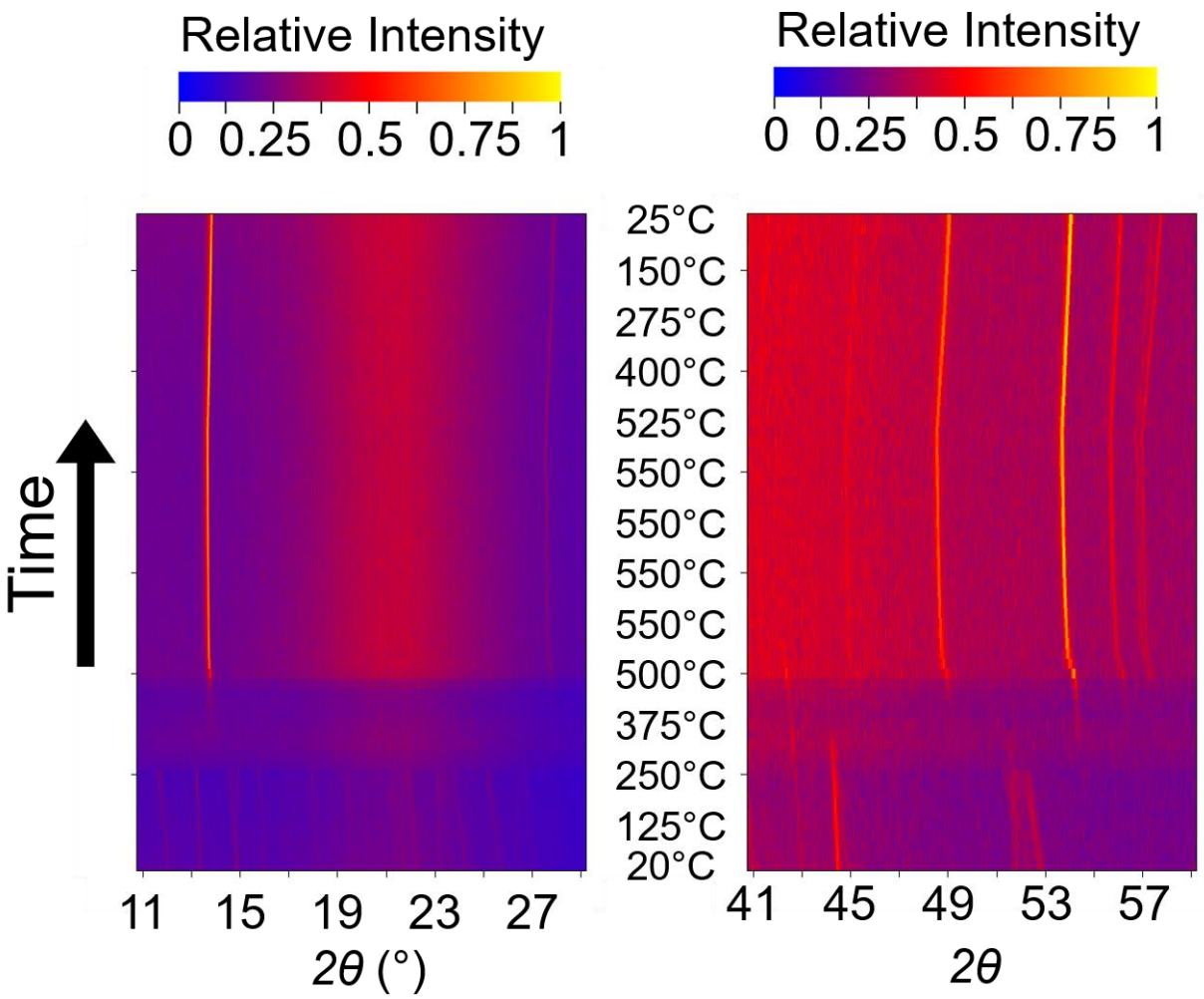

Figure S33. Full range VT-PXRD patterns from the Mn/Ni/P_2S_5 reaction.

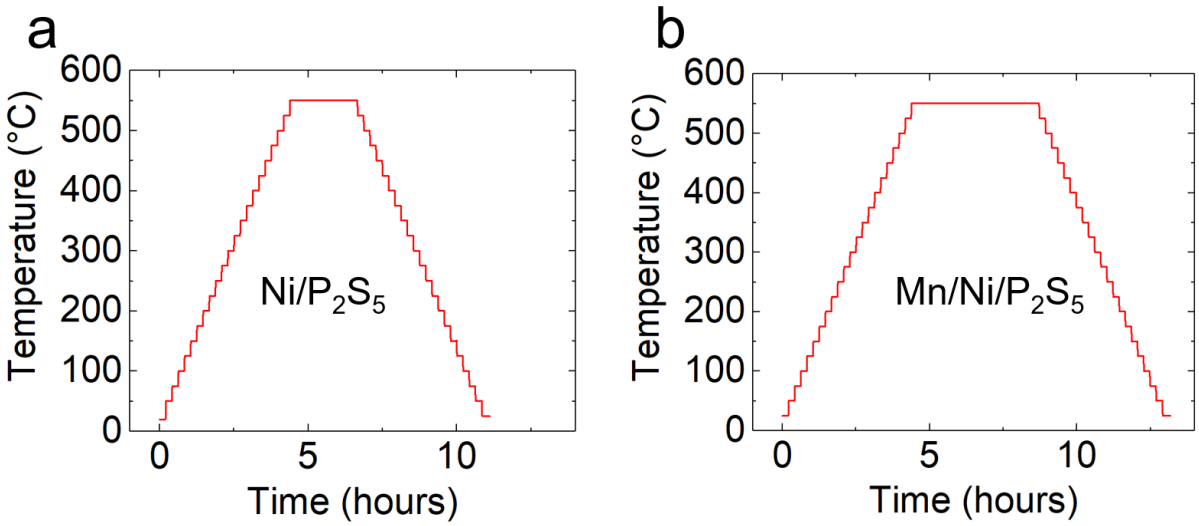

Figure S34. Heating profile used for the variable temperature PXRD measurement of the a.) Ni/P_2S_5 and b.) $Mn/Ni/P_2S_5$ reaction.

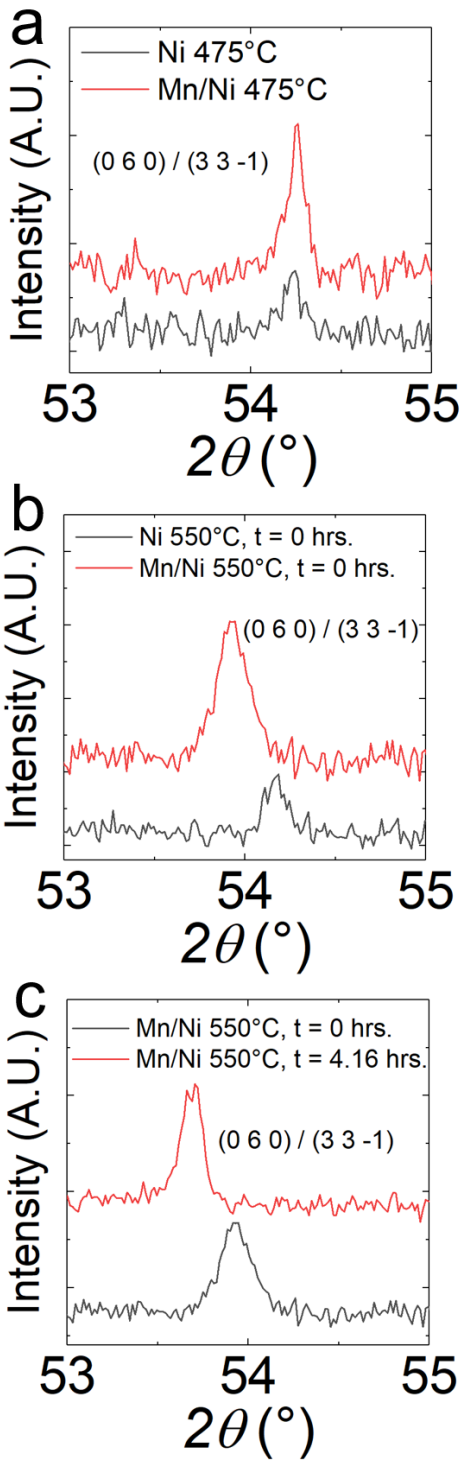

Figure S35. (0 6 0) / (3 3 -1) reflection of the layered thiophosphate phase from the VTPXRD measurement a.) at 475°C compared between both reactions ($2Ni/3P_2S_5$ and $Mn/Ni/3P_2S_5$) and b.) compared between both reactions at 550°C at t = 0 hrs., and c.) compared at 550°C between t = 0 hrs. and 4.16 hrs. for the $Mn/Ni/3P_2S_5$ reaction.

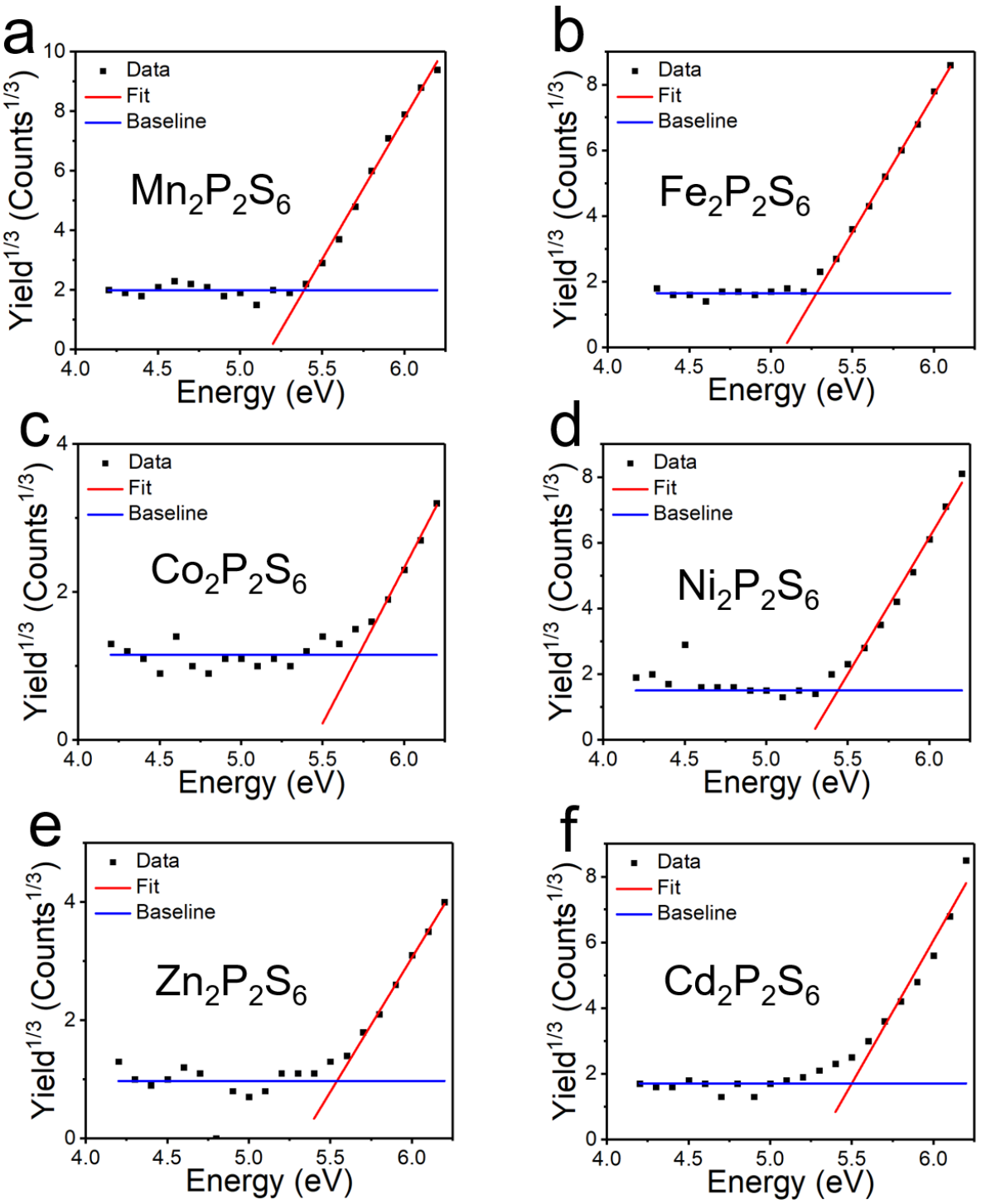

Figure S36 Photoemission yield spectra in air of monometallic thiophosphates, a.) $Mn_2P_2S_6$, b.) $Fe_2P_2S_6$ c.) $Co_2P_2S_6$ d.) $Ni_2P_2S_6$ e.) $Zn_2P_2S_6$ and f.) $Cd_2P_2S_6$.

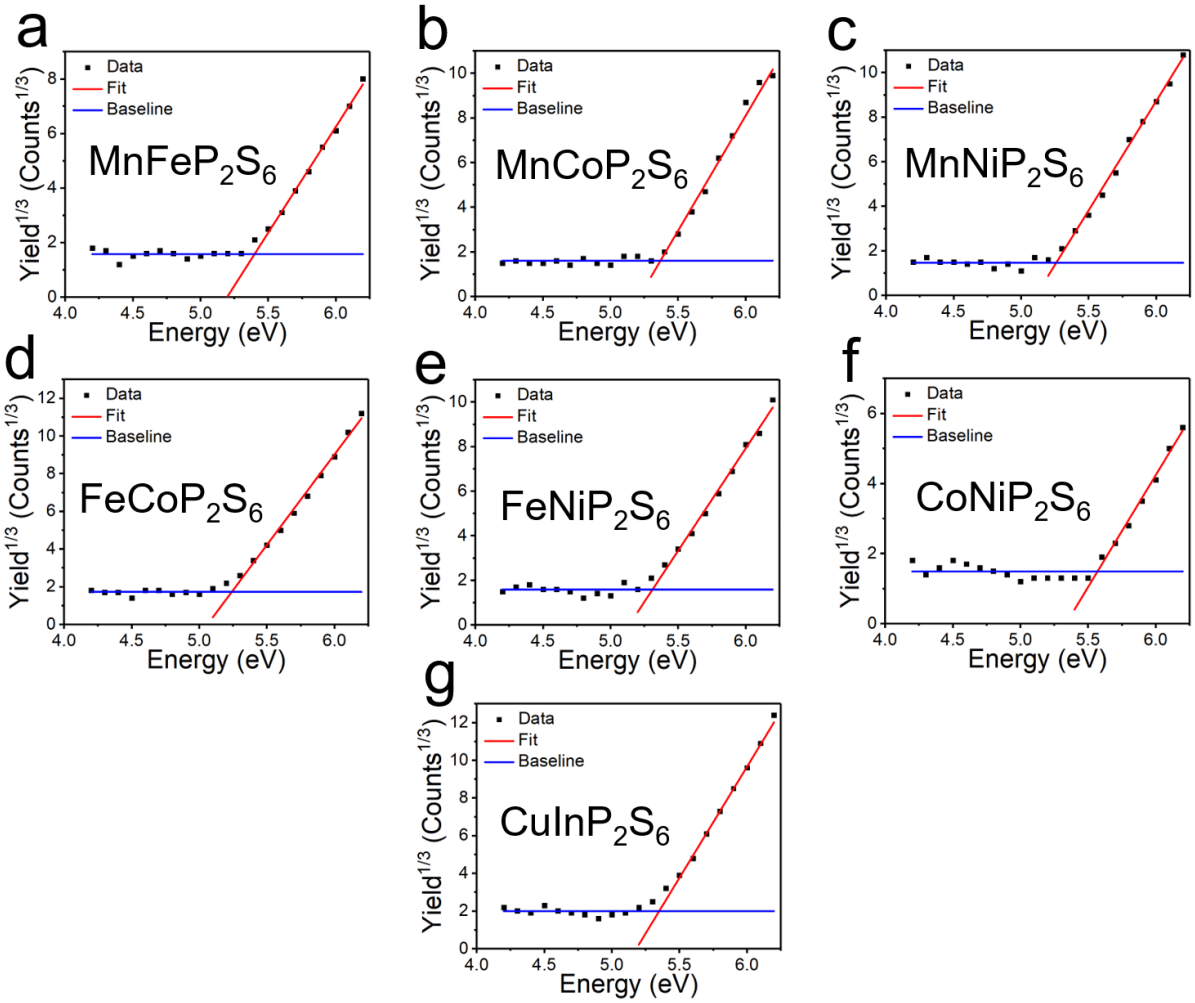

Figure S37. Photoemission yield spectra in air of bimetallic thiophosphates, a.) $MnFeP_2S_6$, b.) $MnCoP_2S_6$ c.) $MnNiP_2S_6$ d.) $FeCoP_2S_6$ e.) $FeNiP_2S_6$, f.) $CoNiP_2S_6$, and g.) $CuInP_2S_6$.

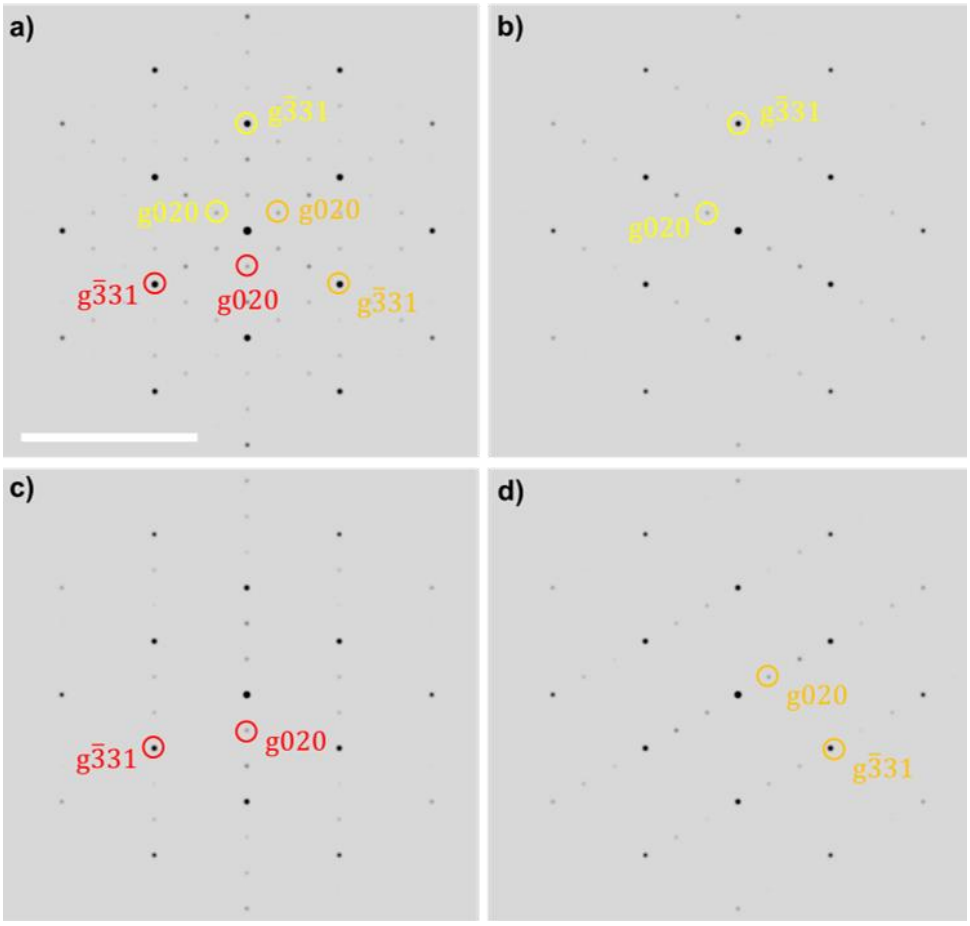

Figure S38. Merged simulated SAED pattern of $Ni_2P_2S_6$ from patterns (b)-(d) along the [103]-zone axis. **(b) ,(c), and (d)** Simulated patterns along the [103]-zone axis where pattern (c) is rotated 120° with respect to pattern (b) and pattern (d) is rotated 240° with respect to pattern (a). The simulated patterns were created with SingleCrystal™.

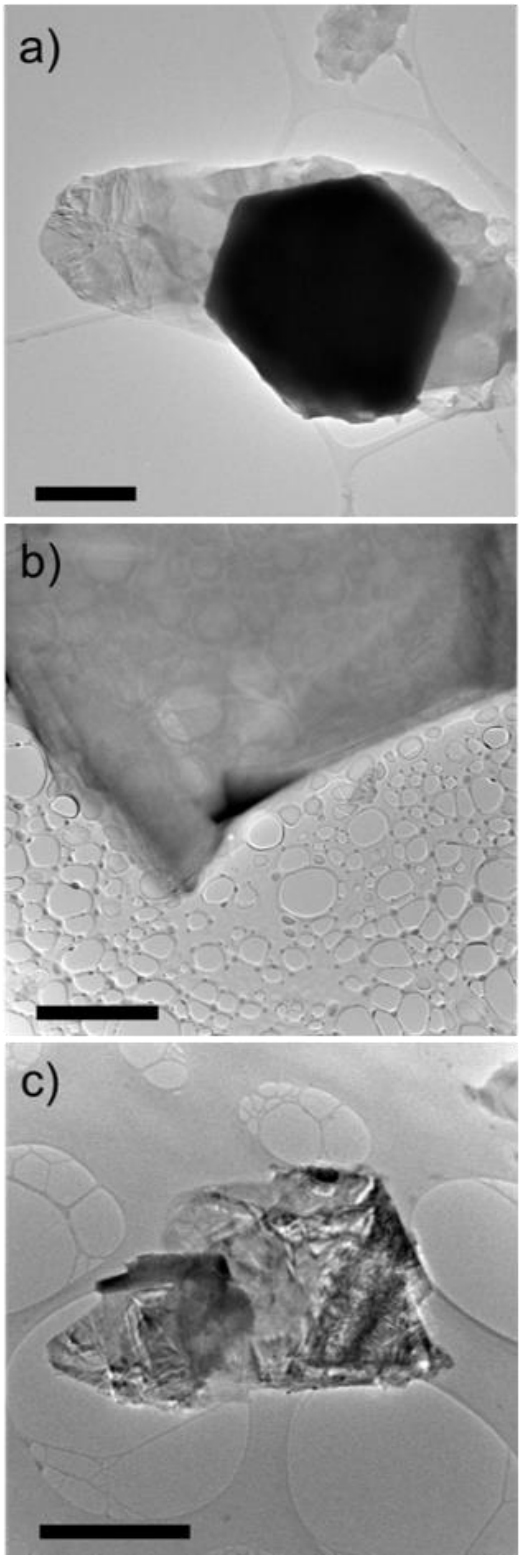

Figure S39. Lower magnification bright-field image of a.) $Ni_2P_2S_6$, b.) $Mn_2P_2S_6$, and c.) $MnNiP_2S_6$. Scale bars are 1um, 5um, and 1um in length, respectively.

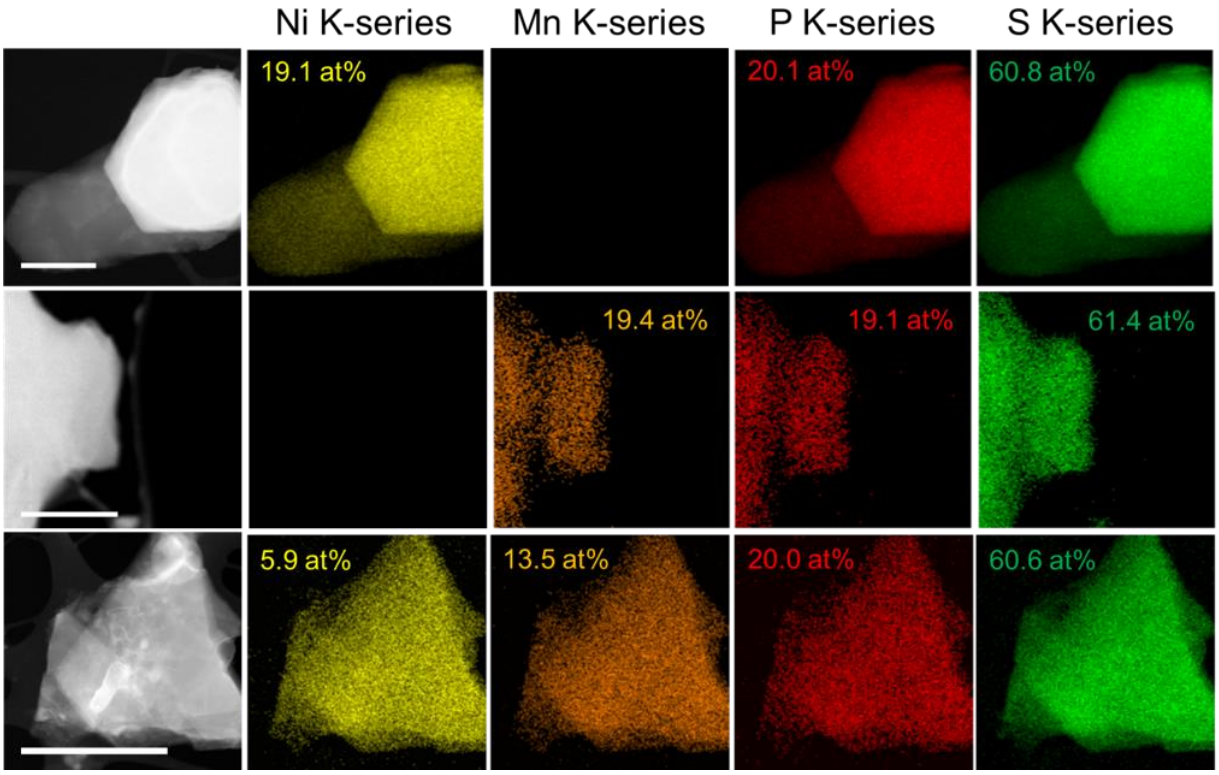

Figure S40. Annular Darkfield STEM images of flakes from the $Ni_2P_2S_6$ (top row), $Mn_2P_2S_6$ (middle row), and $MnNiP_2S_6$ (bottom row) reactions with scale bars corresponding to 1 um and corresponding EDS maps where Ni is denoted in yellow, Mn in Orange, P in red, and S in green. The associated nominally proportional atomic percentages are indicated as well. For the mono cation systems of $Ni_2P_2S_6$ and $Mn_2P_2S_6$ the nominally proportional stoichiometry of each region analyzed agrees with the expected stoichiometry. The alloyed system of $MnNiP_2S_6$ indicates a nominal Ni deficiency relative to Mn as both P and S remain at expected stoichiometry which warrants further study.

References

(1) MacRae, C. F.; Sovago, I.; Cottrell, S. J.; Galek, P. T. A.; McCabe, P.; Pidcock, E.; Platings, M.; Shields, G. P.; Stevens, J. S.; Towler, M.; Wood, P. A. Mercury 4.0: From Visualization to Analysis, Design and Prediction. *J. Appl. Crystallogr.* **2020**, *53*, 226–235. https://doi.org/10.1107/S1600576719014092.

(2) Toby, B. H.; Von Dreele, R. B. GSAS-II: The Genesis of a Modern Open-Source All Purpose Crystallography Software Package. *J. Appl. Crystallogr.* **2013**, *46* (2), 544–549. https://doi.org/10.1107/S0021889813003531.

(3) Kubelka, P.; Munk, F. Ein Beitrag Zur Optik Der Farbanstriche. *Zeitschrift fur Tech. Phys.* **1931**, *12*, 593–601.